Characterization of synaptic transmission in autaptic cultured neurons derived from human induced pluripotent stem cells

Inaugural-Dissertation

to obtain the academic degree

Doctor rerum naturalium (Dr. rer. nat.)

submitted to the Department of Biology, Chemistry, Pharmacy

of Freie Universität Berlin

by

Pascal Fenske

2020

July 2016 – October 2020

Mentor: Prof. Dr. Christian Rosenmund
Department of Neurophysiology, Charité Medical University Berlin

Reviewer 1: Prof. Dr. Christian Rosenmund

Reviewer 2: Prof. Dr. Stephan Sigrist

Defense Date: 12.02.2021

Acknowledgments

First of all, I would like to thank my mentor and supervisor, Prof. Christian Rosenmund, for giving me the opportunity to be part of his fantastic research group and the ability to do my PhD thesis in his lab. I sincerely thank him for his great support and guidance and for allowing me to work independently throughout the entire period of my doctoral studies. I learned from him all necessary electrophysiological skills, but also to be patient especially with complicated or time consuming experiments. He challenged me constantly by letting me question the conceptual “know-how” of every experimental design as well as data interpretation with a broader perspective in mind. In this way, Christian constantly encouraged me to think innovatively and was always available to help me with any problems I encountered. Furthermore, he offered me to work in a laboratory with an international atmosphere and outstanding scientists with whom I could work together the whole time.

I would like to thank Prof. Stephan Sigrist for agreeing to be my second supervisor as part of the Institute of Biology at the Freie Universität Berlin.

I would like to thank all past and present colleagues. Some of them accompanied my journey from the beginning until today, some already left the lab and some just joined. But all of them enriched my life in the Rosenmund lab both professionally and personally. I would like to thank my colleagues for helping me with various problems over the years, having interesting scientific debates, and travelling to conferences together with me. As there are so many of you now, I cannot mention each one by name, but without you I would not have been able to accomplish my doctoral thesis.

Finally, I would like to thank my friends outside the lab and my family. In particular Rike and Jasper, as well as my parents who always supported and cheered me up wherever possible and the great time we have together.

Table of Contents

List of Figures

List of Abbreviations

ADBE	Activity dependent bulk endocytosis
AMPA	α-amino-3-hydroxy-5-methyl-4-isoxazolepropionic acid
AP	Action potential
ATP	Adenosine triphosphate
BDNF	Brain-derived neurotrophic factor
cDNA	complementary DNA
CEM	Clathrin mediated endocytosis
CNS	Central nervous system
CRISPR	Clustered regularly interspaced short palindromic repeats
crRNA	CRISPR RNA
CTL	Control
D-AP5	D-(-)-2-Amino-5-phosphonopentanoic acid
DMEM	Dulbecco′s Modified Eagle′s - Medium
DMEM+	DMEM/F12
DNA	Deoxyribonucleic acid
DPI	Day post induction
EDTA	Ethylenediaminetetraacetic acid
EPSC	Excitatory postsynaptic currents
FCS	Fetal calf serum
GABA	γ-Aminobutyric acid
GFP	Green fluorescent protein
HBS	HEPES-buffered Saline
HEK	Human embryonic kidney cells
iNs	induced Neurons
iPSCs	induced pluripotent stem cells
ISI	Inter-stimulus interval
KD	Knock down
KO	Knock out
L-AP4	L-(+)-2-Amino-4-phosphonobutyric acid

MAP2	Microtubule-associated protein 2
mEPSC	Miniature excitatory postsynaptic currents
mGluRs	Metabotropic glutamate receptors
NBA	Neurobasal-A Medium
NBQX	2,3-Dioxo-6-nitro-1,2,3,4-tetrahydrobenzo[f]quinoxaline-7-sulfonamide
ND	Not detectable
NGN2	Neurogenin-2
NMDA	Methyl-D-aspartic acid
nRRP	Number of vesicles in the RRP
NT	Neurotransmitter
PBS	Phosphate-buffered saline
PBS-T	Tween in PBS
PCR	Polymerase Chain Reaction
PDBu	Phorbol-12,13-dibutyrate
PFA	Paraformaldehyde
PNS	Peripheral nervous system
PPR	Paired-pulse ratio
PVR	Vesicular release probation
QEPSC	Average EPSC charge
QmEPSC	Average mEPSC charge
QRRP	Sucrose response
rcf	Relative centrifugal force
RNA	Ribonucleic acid
RNP	Ribonucleoprotein complex
RRP	Readily releasable pool
RT	Room temperature
SEM	Standard error of mean
sgRNA	short-guided RNA
shRNA	small hairpin RNA
SNARE	Soluble N-ethylmaleimide-sensitive-factor attachment receptor
STP	Short term plasticity
SV	Synaptic vesicle

Syt	synaptotagmin
Syt1	Synaptotagmin-1
tracrRNA	Trans-activating CRISPR RNA
VGlut	Vesicular glutamate transporter
WT	Wild Type

Chapter I

Introduction

Introduction

The nervous system is divided into the central nervous system (CNS) and the peripheral nervous system (PNS). The brain and the spinal cord are the primary component of the CNS. The PNS is formed by nerves and ganglia that connect organs and extremities. The primary function of the PNS is to send information to the CNS where it is processed to coordinate the activity of the entire body. The PNS connects the CNS to the limbs and organs and builds up a communication system going back and forth between the brain and the rest of the body. Information is transmitted and interpreted by a complex network of nerve cells in the brain, which are known as neurons. When neurons are electrically excitable specialized connections called synapses enable the transfer of information between neurons (Kandel, Schwartz et al. 2000, Hammond 2001).

The Chemical Synapse

Neurons are connected to each other by electrical and chemical synapses. Electrical synapses are linked by gap junctions which permit bidirectional passive flow of current between the pre- and postsynaptic membrane. The extracellular synaptic distance is very small, around 3 nm and the transmission speed of the signal is about ten times faster than chemical synapses (Larsen 1977). Electrical transmission is known to occur in the retina, inferior olive and the olfactory bulb. Furthermore, electrical synapses are more abundant in invertebrates and cold-blooded vertebrates (Hormuzdi, Filippov et al. 2004, Pereda 2014).

Chemical transmission occurs between synaptic terminals from axons and the dendrite or soma of a second neuron, muscle fiber or gland cell (Pereda 2014). At these synapses, the electrical signal is transmitted along an axon by voltage-gated ion channels to the axon terminal, where the action potential (AP) leads to the release of neurotransmitter (NT) into the synaptic cleft. The release of the NT is the chemical signal. The released NTs bind to receptors on the post synaptic cell, this interaction triggers the opening of ionic

channels on the membrane. This causes an influx of ions across the membrane or modulates the production of chemical messengers. This influx changes the postsynaptic membrane potential, which allows the regeneration of an electrical signal. For a functional network this process needs to be rapid, reliable and highly adaptable (Kandel, Schwartz et al. 2000, Hammond 2001). In this work we will focus mainly on the process of presynaptic NT release which will be described in more detail in the following paragraph.

The Synaptic Vesicle Cycle

In the presynaptic terminal, NTs are stored in synaptic vesicles (SVs) that can fuse with the plasma membrane to release their content. The precise timing of the release is very important for normal synaptic function. Furthermore, during neuronal activity efficient endocytic membrane retrieval is required to keep the membrane surface area constant and reformation of SVs is needed to replenish the SV pool (Sudhof and Jahn 1991, Kononenko, Puchkov et al. 2014). Hence, the SVs undergo a trafficking cycle (Figure 1) (Sudhof 2004).

Before SV exocytosis can occur, SVs need to be ready for fusion with the plasma membrane. The fusion of the SVs occurs in a specialized area of the presynaptic plasma membrane, the active zone. The active zone can be identified under the electron microscope directly at the synaptic cleft. This structure results from the accumulation of cytoskeleton-associated proteins forming the cytomatrix of the active zone. Different non-membrane proteins at the active zone create a homogeneous single complex by binding to each other. These are multidomain proteins, namely Munc13s and RIMs (Brose, Hofmann et al. 1995, Wang, Okamoto et al. 1997, Wang, Sugita et al. 2000, Dresbach, Qualmann et al. 2001, Wang and Sudhof 2003). The proteins interact with each other and other synaptic components such as Piccolo and Bassoon, that are large homologous proteins forming part of the cytomatrix (Cases-Langhoff, Voss et al. 1996, tom Dieck, Sanmarti-Vila et al. 1998); Coiled-coil proteins such as ERCs, RIM-BPs and α-liprins, bind to RIMS, ERCs

and receptor protein tyrosine phosphatases (Serra-Pages, Medley et al. 1998, Wang, Sugita et al. 2000, Ohtsuka, Takao-Rikitsu et al. 2002, Wang, Liu et al. 2002, Ko, Na et al. 2003).

With the help of numerous proteins, the SV is first tethered in close vicinity to the active zone, docked in direct contact with the plasma membrane and "waiting" for fusion (Dresbach, Qualmann et al. 2001, Jahn and Fasshauer 2012). After docking, a priming reaction leaves the SV in a metastable state, which allows it to be ready to release its cargo upon Ca^{2+} influx. Membrane fusion requires energy which is provided by the SNARE proteins (Soluble N-ethylmaleimide sensitive factor Attachment protein Receptor) (Weber, Zemelman et al. 1998). Prior to the Ca^{2+} influx a *trans*-SNARE complex is formed by the SV localized SNARE protein synaptobrevin-2/VAMP2, the plasma membrane associated syntaxin-1 and SNAP-25 (Sudhof and Rizo 2011). The binding of Ca^{2+} to the Ca^{2+}-sensing protein synaptotagmin (Syt) leads to conformational changes in Syt and within 100 μs after the arrival of an AP the fusion of SVs occur (Rizo and Rosenmund 2008).

Most vesicles that are docked and primed belong to the readily-releasable pool (RRP) (Denker and Rizzoli 2010). These SVs are immediately available upon stimulation and can be rapidly depleted with high frequency stimulation. Two other SV pools can be distinguished: the recycling pool and the reserve pool. The SVs from the reserve pool are rarely utilized during physiological activity while the recycling pool maintains release in response to moderate stimulation and is refilled by newly recycled vesicles (Rizzoli and Betz 2005).

Following exocytosis SVs need to be regenerated. Membrane originating from SVs are retrieved and parts of the protein release machinery is recycled and sorted. Finally, the newly formed SVs are filled with NT (Rizzoli 2014). The vesicular ATPase, located in the vesicle membrane, hydrolyzes adenosine triphosphate (ATP) in order to pump protons into SVs, thus creating both a proton gradient and an electrical potential across the vesicular membrane. This electrochemical gradient is further used by NT transporters, like vesicular glutamate transporter (VGlut) and Vesicular GABA transporter,

to pump NTs into the vesicles (Hammond 2001, Chanaday, Cousin et al. 2019).

Several mechanisms have been proposed for the recovery of SVs at the synapse: fusion pore closure “kiss and run”, clathrin mediated endocytosis directly from the plasma membrane (CME), activity-dependent bulk endocytosis (ADBE) and ultrafast endocytosis. The “kiss and run” model proposes that SVs are quickly recycled by a direct reversal of the exocytotic process without an intermixing between the SV and presynaptic plasma membrane (Valtorta, Meldolesi et al. 2001, Alabi and Tsien 2013).

During CME, clathrin-coated pits invaginate from the membrane surface and with the help of other proteins pinch off from the membrane. The clathrin coat subsequently falls off and these vesicles can be directly filled with NT (Conner and Schmid 2003, Doherty and McMahon 2009, Saheki and De Camilli 2012).

An alternative proposed mechanism of endocytosis during more intense neuronal activity is the ADBE (Clayton and Cousin 2009, Morton, Marland et al. 2015). In ADBE large areas of the plasma membrane invaginates to form bulk endosomes from which SVs are generated to replenish the recycling pool (Wenzel, Morton et al. 2012, Morton, Marland et al. 2015).

Recently a new mechanism, ultrafast endocytosis, has been proposed for the recycling of SVs. In a clathrin-independent manner, a single large endocytic vesicle (50-100 ms) is retrieved after vesicle fusion. Dynamin is required for the step of invagination. Clathrin is required later for the formation of SVs from the endosome (Watanabe, Rost et al. 2013, Watanabe, Trimbuch et al. 2014, Delvendahl, Vyleta et al. 2016).

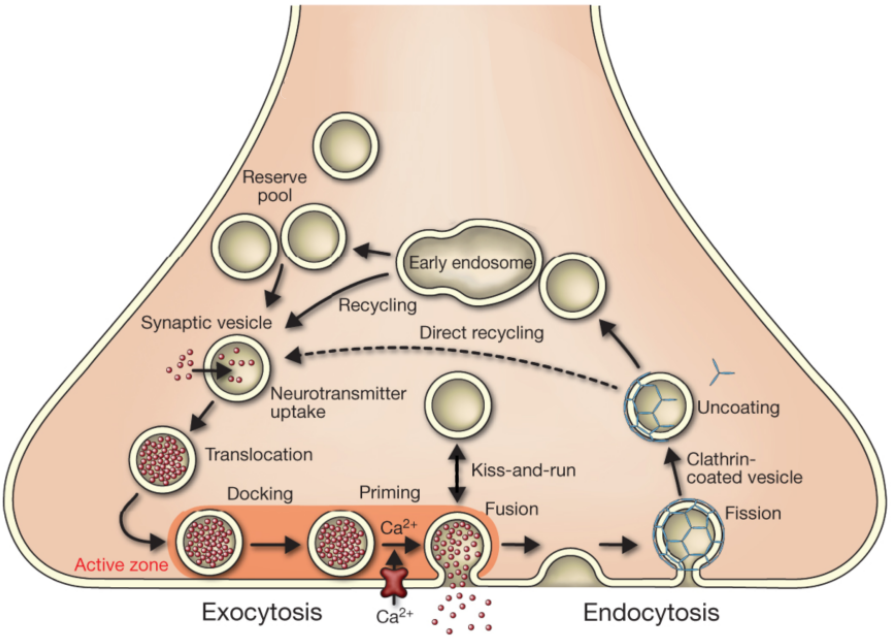

Figure 1: The synaptic vesicle cycle.
Vesicles are filled with neurotransmitters. The SV docks at the plasma membrane in the active zone and becomes primed. Upon calcium influx fusion occurs and neurotransmitters are released. After this the membrane is retrieved by endocytosis and the SV undergoes a recycling pathway (modified from (Jahn and Fasshauer 2012))

Studying NT release

Work by Katz, Eccles and others using electrophysiological measurements showed the central importance of synapses for brain function and characterized the basic mechanisms involved in synaptic transmission. Over the last decades, many molecular functions of synapses have been understood and elucidated. Moreover, technical advances that went beyond the classical approaches have provided more details and insights. These include capacity measurements of exocytosis directly at the presynapse and the controlled release of Ca^{2+} by uncaging experiments (Neher and Marty 1982, Delaney and Zucker 1990). Other methods are based on imaging analysis such as the use of FM1-43 or Synapto-pHluorin. They provide the possibility to visualize the release of SVs as well as their internalization and reacidification during endocytosis (Rizzoli and Betz 2005).

Many studies aimed to elucidate motives for circuits such as feedforward, feedback, recurrent and lateral inhibition and excitation (Douglas and Martin 2007, Yuste 2015). One of the simplest circuit motives imaginable, namely the synaptic connection of a neuron with itself, was only recognized relatively late. The term "autapse" entered the encyclopedia of neuroscience in 1972 (Van Der Loos and Glaser 1972).

The Autaptic culture system

Autaptic cultures, in which single neurons grow in isolation on astrocytic microislands and form synapses exclusively with themselves (Bekkers and Stevens 1991), provide an experimental system with access to detailed characteristics underlying synaptic transmission. This system allows for the quantitative assessment of input and output properties of individual neurons, both in morphological and in functional experiments (Sampathkumar, Wu et al. 2016). In addition, parameters such as vesicle fusogenicity, vesicular release probability (P_{VR}), short-term plasticity and SV pool sizes can be assessed (Figure 2) (Basu, Betz et al. 2007, Trimbuch, Xu et al. 2014). The autaptic culture system has proven particularly valuable in the analysis of presynaptic

release mechanisms, including docking/priming and the functionality of the fusion machinery (Rhee, Betz et al. 2002, Varoqueaux, Sigler et al. 2002, Basu, Shen et al. 2005, Rhee, Li et al. 2005, Li, Shin et al. 2006, Arancillo, Min et al. 2013, Schotten, Meijer et al. 2015, Camacho, Basu et al. 2017, Lipstein, Verhoeven-Duif et al. 2017), as well as developmental phenotypes (Sampathkumar, Wu et al. 2016). Moreover, it has been a powerful tool to distinguish between cell-autonomous and non-cell-autonomous regulatory processes (Chang, Trimbuch et al. 2014, Sampathkumar, Wu et al. 2016) and to describe the cellular phenotypes associated with neurological disorders, e.g. Rett syndrome (Chao, Zoghbi et al. 2007, Chao, Chen et al. 2010, Sampathkumar, Wu et al. 2016), and neurodegenerative diseases such as Alzheimer's Disease (Ting, Kelley et al. 2007, Pratt, Zhu et al. 2011).

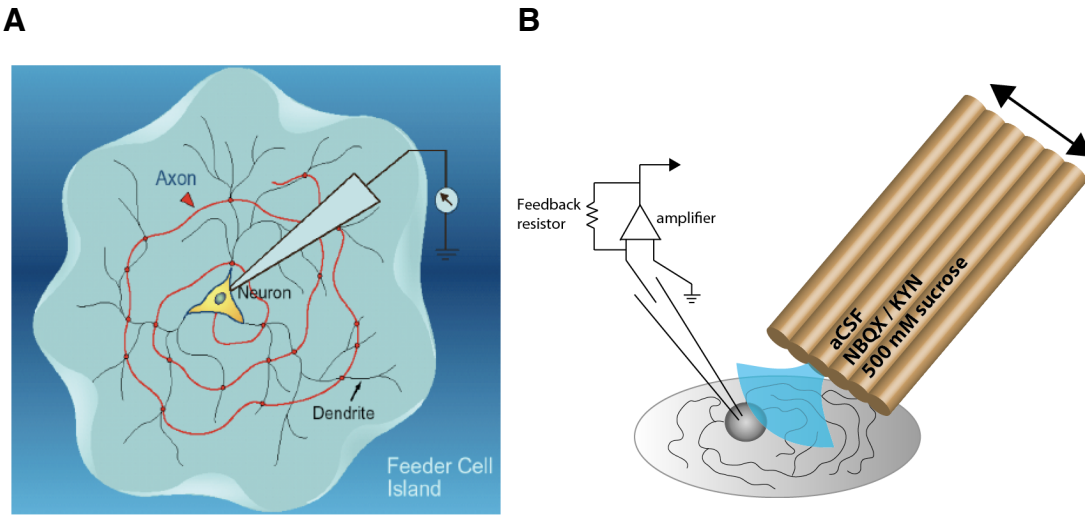

Figure 2: The autaptic cell culture system
A) *A schematic of the autaptic culture system with a neuron sitting on a feeder island. The dendrites are confined to the borders of the island and are making repeated autaptic connections to the axon. Credit: Christian Rosenmund.* ***B)*** *A schematic of our fast flow system. The position of the opening of each pipe is centered to the soma (aCSF: artificial cerebrospinal fluid; NBQX: 2,3-Dioxo-6-nitro-1,2,3,4-tetrahydrobenzo[f]quinoxaline-7-sulfonamide; KYN: kynurenic acid). With the help of a computer controlled stepper and valve bank, the solution which is needed can be applied to the patched cell.*

Human neurons as model system

In order to understand the neuronal function of humans, it is crucial to gain knowledge of how human synapses function. For this purpose, new approaches are needed to define unique properties of human synapses.

Progress in the analysis of the human genome has led to the discovery of many new monogenetic disorders of the CNS. While this has helped in the diagnosis of rare diseases, understanding the underlying pathophysiology is a greater challenge. Research on model organisms including the worm, fly, fish and rodent has been used with good success to date to summarize both organismic and cellular aspects of the genetic defects (Hofker, Fu et al. 2014). However, it is still unclear how well these model organisms reflect the situation in human patients. Similarly, the mechanisms of NT release have been studied for decades in different invertebrate and vertebrate model systems (Fatt and Katz 1951, Furshpan and Potter 1959, Jan, Jan et al. 1977, Borst, Helmchen et al. 1995, Moyer and Brown 1998, Zhen and Jin 1999, Bischofberger, Engel et al. 2006). The rodent model system has proven especially valuable for modeling monogenic human diseases and understanding their underlying causes (Comery, Harris et al. 1997, Jiang, Armstrong et al. 1998, Asaka, Jugloff et al. 2006, Hung, Futai et al. 2008, Chao, Chen et al. 2010, Michalon, Sidorov et al. 2012, Schmeisser, Ey et al. 2012, Kouser, Speed et al. 2013, Fromer, Pocklington et al. 2014, Purcell, Moran et al. 2014, Duffney, Zhong et al. 2015).

Recent technological advances now provide access to human neurons through the establishment of induced pluripotent stem cells (iPSCs) and neuronal differentiation protocols (Chambers, Fasano et al. 2009, Shi, Kirwan et al. 2012, Zhang, Pak et al. 2013, D'Aiuto, Zhi et al. 2014, Gunhanlar, Shpak et al. 2018). Alternatively, direct conversion of fibroblasts into neurons can be performed (Vierbuchen, Ostermeier et al. 2010, Colasante, Lignani et al. 2015).

Two potential advantages of cultured human neurons are that first they better reflect human biology than animal models and second they are suitable

for the study of complex genetic diseases by employing iPSCs generated directly from the affected patient. Importantly, the usage of iPSCs makes the replacement of transgenic animal lines possible. To date, transgenic animals are still the basis for research in the field of synaptopathies (Hook, Brennand et al. 2014, Mertens, Wang et al. 2015, Pak, Danko et al. 2015, Yi, Danko et al. 2016, Young-Pearse and Morrow 2016, Forrest, Zhang et al. 2017).

Induced Neurons (iNs) possess great potential for studying the basic mechanisms of NT release in a controlled genetic background (Pak, Danko et al. 2015, Patzke, Han et al. 2015). Recent studies have investigated evoked NT release in human iNs grown in mass culture (Zhang, Pak et al. 2013, Pak, Danko et al. 2015, Patzke, Han et al. 2015, Patzke, Acuna et al. 2016, Gunhanlar, Shpak et al. 2018). However, the depth of analysis of synaptic properties and parameters has been limited due to the complex network formed in this conventional culture system.

So far, the poor survival rate of solitary human iNs, which is necessary to obtain autaptic cultures, and their long differentiation time in comparison to rodent primary neurons has hampered the accessibility of these cultures to experimental assessments. Moreover, the research community is still largely critical of this approach and continue to rely on established animal models.

Aims of this study

Synaptic transmission has been studied over the last decades mainly in different model organisms, including invertebrates and vertebrates. Autaptic cultures for the investigation of synaptic transmission were performed mainly on neurons of mice and rats. One reason for this was that the accessibility of human neurons was restricted.

Our primary aim was to transfer the increasing number of studies on human iNs performed in conventional mass cultures to the autaptic model for the first time. For this purpose, we developed a novel two phase culture system for human autaptic cultures.

The second aim was to characterize basic morphology parameters including axon and dendrite length as well as synapse formation by immunocytochemistry. In the next step we wanted to characterize the basic physiological parameters to access the synaptic input and output function, and determine synaptic efficacy. Therefore, we performed electrophysiological recordings including the assessment of modulation of synaptic responses by endogenous and exogenous modifiers of synaptic transmission.

The third aim was to show an application-based validation of the autaptic human neurons from human iPSC. This would allow us to demonstrate the reliability of our cell culture system of human neurons as a replacement of the animal autaptic model system to study synaptic transmission. As a proof of principle, we first used a small hairpin ribonucleic acid (shRNA) based knocked down of UNC 13-A in an acute manner. As a second approach we generated a human stem cell line deficient for Synaptotagmin 1. We therefore can test the sensitivity of human autaptic cultures for the investigation of synaptic transmission in comparison to the known effects of Synaptotagmin 1 deficiency in the rodent models.

Chapter II

Material and Methods

Materials and Methods

Animals

C57BL6/N mice were used in this work to obtain astrocyte enriched primary cultures. All procedures to maintain and use mice were approved by the Animal Welfare Committee of the Charité Medical University and the Berlin State Government (license no. T0220/09).

Cell culture

Maintenance of iPSC

IPSCs were obtained from three independent lines provided by the Berlin Institute of Health Core Facility Stem Cells (Berlin, Germany): The iPSC line BIHi001-A (https://hpscreg.eu/cell-line/BIHi001-A) was derived from human foreskin fibroblasts using Sendai virus vectors (CytoTune-iPSC reprogramming kit, ThermoFisher Scientific, Waltham, MA, USA). The iPSC line BIHi004-A (https://hpscreg.eu/cell-line/BIHi004-A) was derived from human fibroblasts using episomal vectors (Epi5 Episomal iPSC Reprogramming Kit, ThermoFisher Scientific). The iPSC line BIHi005-A (https://hpscreg.eu/cell-line/BIHi005-A) was derived from fibroblast of dermis in the OLS using Sendai virus vectors (Miltenyi mRNA, Miltenyi Biotec, Germany). IPSCs were maintained as feeder-free cells in StemFlex medium (ThermoFisher Scientific) in a standard incubator (37 °C, 5 % CO_2).

Preparation of microdot patterned glass coverslips

Glass coverslips (30 mm diameter, (Glaswarenfabrik Karl Hecht, Germany)) were cleaned with 1 M HCl (Carl Roth, Germany) on a shaker overnight, rinsed three times with ddH_2O and finally stored in 95 % ethanol (Carl Roth, Germany). To remove the alcohol coverslips were briefly flamed before placing them into 6-well-plates (Corning, Inc, USA). In a next step, glass coverslips were then coated with liquefied 0.15 % agarose type IIa (Sigma-Aldrich, Germany). The coating forms a thin layer on which cells are reluctant

to attach. Using a custom-built stamping machine uniformly sized microislands (~200 μm diameter, 500 μm space between spots) of a permissive growth solution (collagen/poly-D-lysine) (Gibco Life Technologies, Germany and Sigma Aldrich, Germany) were applied to the agarose coated glasses. Plates with micropatterned glasses were sterilized using ultraviolet light and stored at room temperature (RT) until further use.

Preparation of astrocytes

Astrocytes were obtained from newborn C57/BL6-N mice. Briefly, animals were sacrificed and brains were removed. Brains were quickly transferred into 4 °C cooled Hank‘s Balanced Salt Solution (HBSS, Gibco Life technologies, Germany). Under a binocular microscope the cortices were dissected and the meninges removed. Cortices were digested for 20 minutes at 37 °C in a shaker at 800 revolutions per minute with 800 μl of 0.05 % trypsin-EDTA (ethylenediaminetetraacetic acid). Digested cortices were placed in DMEM (Dulbecco’s Modified Eagle’s - Medium) full medium and triturated to obtain a suspension of dissociated cells. 400 μl cell suspension were placed into a flask (surface area 75 cm^2) (Corning, Inc, USA) containing 13 ml pre-warmed DMEM full medium. Flasks were stored in an incubator (37 °C, 5 % CO_2) to allow the astrocytes to grow for 1 to 2 weeks. After reaching 80 % confluency, astrocyte flasks were vortexed for approximately 1 minute. Cells were washed with phosphate-buffered saline (PBS) and detached from the surface by adding 5 ml of 0.05 % trypsin-EDTA. 7 ml DMEM full medium was added to stop digestion and cells were dissociated and transferred into tubes for centrifugation for 5 min at RT and 300 relative centrifugal force (rcf). After centrifugation the cells were counted and ready for plating. Astrocytes were plated at a density of 5 x 10^3 cells per cm^2 onto the microdot-coated coverslips one week before iNs were added. For the addition of astrocytes during the induction process the same protocol to detach the cells was used. After the centrifugation the cell pellet was resuspended in Neurobasal A (NBA) + media and the cell suspension was added to the human iNs.

Virus Generation

Lentiviruses were produced by cotransfection of HEK293T cells with 3.9 µg of pRSV-REV (Addgene Plasmid #12253), 8.1 µg pMDLg/pRRE (Addgene Plasmid #12251) packaging plasmids, 6 µg of envelope plasmid VSVg (Addgene Plasmid #12259)) and 12 µg complementary DNA (cDNA) transfer plasmids containing the construct of interest (e.g. Tet-O-FUW or FUGW) in a T75 flask using calcium phosphate. 24 h before transfection 6.8 x 10^6 HEK (Human embryonic kidney cells) cells were seeded in the T75 bottle. One hour prior to transfection, medium was changed for new DMEM with 10 % fetal calf serum (FCS). The required plasmids (see above) were mixed with 111.6 µl 2M CaCl and 768 µl H2O. This mixture was then added slowly and dropwise to 900 µl 2 x HBS (HEPES (4-(2-hydroxyethyl)-1-piperazineethanesulfonic acid) -Buffered Saline) and shaken horizontally for 10 sec in a 14 ml round bottom tube. After 20 minutes incubation at RT without shaking, the transfection mix was added to the HEK cells. 5 h later the media was replaced with DMEM containing 10 % FCS and cells were incubated at 37 °C in the incubator.

Supernatants containing lentivirus particles were harvested 48 h after transfection and purified using Amicon Ultra-15 Centrifugal Filter units Ultracel-100K (Merck Millipore, MA, USA). Thus the 12 ml of the supernatant were concentrated to 200 µl. The virus was then stored in 20 µl aliquots at -80 °C until use. Only virus batches with > 90 % infection efficiency, as assessed by green fluorescent reporter expression (FUW-eGFP) or by 90 % survival cells by brightfield puromycin resistance (FUW-TetO-Ngn2-T2A-Puro), were used for experiments. cDNA constructs for rtTA (FUW-rtTA), Ngn2 (FUW-TetO-Ngn2-T2A-Puro) and eGFP (FUW-eGFP) were kindly provided by Thomas C. Südhof, (Stanford University School of Medicine, USA). For Unc13A knockdown (KD) a synthetic shRNA oligonucleotide (sequence: 5’ ggacaccatcaagcaatat ttcaagaga atattgcttgatggtgtcc ttttttccaa 3’) was inserted into a FUGW shuttle vector (Lois, Hong et al. 2002) containing a U6 promoter and a synapsin promoter driven NLS-RFP reporter gene.

Generation of iN Cells from human iPSCs

Excitatory human iNs were produced essentially as described previously (Zhang, Pak et al. 2013). On day -1, seeded iPSCs were dissociated with Accutase cell dissociation reagent (ThermoFisher Scientific) and re-seeded on 6-well plates coated with Matrigel (Corning) (300 K per well) in StemFlex Medium containing 2 μM Thiazovivin (Tocris, Bristol, UK) and lentiviral particles for transduction of Neurogenin-2 (NGN2), rtTA and eGFP. On day 0 the culture medium was changed to DMEM/F12 (DMEM+) (ThermoFisher Scientific), supplement with N-2 (ThermoFisher Scientific), non-essential amino acids (ThermoFisher Scientific), human Brain-derived neurotrophic factor (BDNF) (10 mg/l, PeproTech, Hamburg, Germany), human NT-3 (10 mg/l, PeproTech), mouse laminin (0.2 mg/l, ThermoFisher Scientific) as well as doxycycline (2 μg/ml, Sigma Aldrich) to induce TetO-dependent gene expression. Doxycycline was included in all media until the end of the experiments. On day 1, the medium was changed as described above and additionally 0.5 mg/l puromycin was included to select for iNs. This was achieved as the NGN2 plasmid contains a puromycin resistance cassette. On day 3, the medium was replaced with NBA+ medium (ThermoFisher Scientific), which included B-27 supplement (ThermoFisher Scientific), GlutaMAX (ThermoFisher Scientific) human BDNF (10 mg/l), human NT-3 (10 mg/l), mouse laminin (0. 2 mg/l), cytosine β-D-Arabinofuranoside (Ara-C) (2 mg/ml, Sigma Aldrich) and doxycycline (2 μg/ml). Additionally, mouse astrocytes were added at the density of 3 x 10^5 cells/cm^2 at the same time period. From day 7 on, half of the medium in each well was replaced every 5 days by NBA+ medium containing B-27 supplement, GlutaMAX, doxycycline (2 μg/ml) and 2.5 % fetal bovine serum (Pan Biotech, Aidenbach, Germany). After 50-70 days cells were washed twice with 0.5 mM EDTA/PBS (ThermoFisher Scientific) and dissociated with Accutase Cell Dissociation Reagent (twice for 7 min at 37 °C). Only the GFP-positive cells were counted in a hemocytometer under a fluorescence microscope and seeded at a density of 4 K per well on astrocyte feeder micro-islands glass to obtain induced

human neuronal autaptic cultures. Cells on microislands were seeded in media containing NBA for human iN mass cultures supplemented with human BDNF (10 mg/l), human NT-3 (10 mg/l) and mouse laminin (0. 2 mg/l). These cultures were maintained in a humidified incubator (37 °C and 5 % CO2) for 13-21 days.

Media and cell culture solutions

DMEM full

Component	Volume (ml)
Fetal calf serum	50
Penicillin / Streptomycin (10.000 U/ml; 10.000 µg/ml)	5
DMEM + GlutaMAX	500

PBS/EDTA

Component	Amount
PBS	500 ml
0.5 M EDTDA pH 8.0	500 µl

StemFlex

Component	Amount
StemFlex medium	450 ml
StemFlex supplement	50 ml

2x HBS pH 6.95

Component	Amount
NaCl	16 g
HEPES	10 g
Glucose	2 g
KCl	0.74 g
Na_2HPO_4	0.212 g
H_2O	Add to 1000 ml

DMEM+ medium

Component (unit)	Volume (µl)
N2	500
NEAA	500
BDNF (10 µg/ml)	50
Laminin (1000 µg/ml)	10
NT3 (10 µg/ml)	50
Doxycycline (1000 µg/ml)	100
DMEM/F12 (ml)	49,0 ml

NBA+ medium

Component (unit)	Volume (µl)
B27	1000
GlutaMAX	500
BDNF (10 µg/ml)	50
Laminin (1000 µg/ml)	10
NT3 (10 µg/ml)	50
Ara-C (50000 mg/ml)	2
Doxycycline (1000 µg/ml)	100
NBA	48,5 ml

NBA for human iN mass culture

Component (unit)	Volume (ml)
B27	10
Glutamax	5
FBS	12,5
Penicillin / Streptomycin (10.000 U/ml; 10.000 µg/ml)	5
Doxycyclin (1000 µg/ml)	1
NBA	500

Immunocytochemistry

Autaptic human induced neuronal cultures were fixed between day 80 and 121 in 4 % paraformaldehyde (PFA, Sigma Aldrich) / 4 % sucrose (Sigma Aldrich) in PBS (Merck Millipore) for 10 min at RT and washed three times with PBS. Cells were permeabilized for 15 min in PBS with 0.1 % Tween-20 (Carl-Roth GmbH + Co. KG, Karlsruhe, Germany) (PBS-T), incubated in quenching solution (100 mM glycine in PBS) for 30 min and blocked in 5 % normal donkey serum (Jackson ImmunoResearch Inc., West Grove, PA, USA) (in PBS) for 1 hour at RT. Autaptic human iNs were incubated with primary antibodies in blocking solution over night at 4 °C. The following primary antibodies were used: chicken anti-microtubule-associated protein 2 (MAP2) (1:2000; Merck Millipore, AB5543), mouse anti-pan-axonal neurofilaments (SMI-312; 1:1000; Covance inc., Princeton, NJ, USA); mouse anti-synaptotagmin-1 (1:200; Synaptic Systems, Göttingen, Germany, 105 011). After primary antibody incubation, human iNs were washed three times with PBS-T, and secondary Alexa-Fluor 405 or 647 (1:500; Jackson ImmunoResearch Inc.) antibodies were added for 1 h at RT in PBS-T. Cells were washed twice in PBS-T and once in PBS before they were mounted on glass slides with Mowiol (ThermoFisher Scientific).

Morphological analysis

For morphological analysis of autaptic human induced neuronal cultures, stacks of 16-bit fluorescence images were acquired on an Olympus IX81 inverted fluorescence microscope equipped with a 10 X or 20 X objective (neurite length analysis) or a 60 X water immersion objective (synaptic density analysis). Images were acquired with a CCD camera (Princeton MicroMax; Roper Scientific, Trenton, NJ) using MetaMorph software (Molecular Devices, Sunnydale, CA, USA). All images were analyzed using ImageJ software (National Institutes of Health, Bethesda, MD, USA). For each image stack maximum intensity projection were generated. Uniform background subtraction and optimal threshold adjustment was performed on all images.

Quantification of MAP2-positive or neurofilament (SMI312)-positive processes with the NeuronJ plugin was used to determine total dendritic and axonal lengths, respectively. The density of synaptophysin-positive punctae overlapping with MAP2-positive dendrites was determined using a custom-written ImageJ plugin. Two independent cultures were imaged and analyzed per group for every experiment.

Electrophysiology

Whole-cell patch-clamp recordings were performed in single human iNs between day 63 and 91 post neuronal induction at RT using a Multiclamp 700B amplifier (Molecular Devices). The series resistance was compensated by 70 % and only cells with series resistances of < 12 MΩ were analyzed. Data were acquired at 10 kHz using pClamp 10 software (Molecular Devices) and filtered using a low-pass Bessel filter at 3 kHz. Data were analyzed offline using AxoGraph X (AxoGraph Scientific). The patch pipette solution contained 136 mM KCl, 17.8 mM HEPES, 1 mM EGTA, 0.6 mM $MgCl_2$, 4 mM ATP-Mg, 0.3 mM GTP-Na, 12 mM phosphocreatine, and 50 units/mL phosphocreatine kinase (300 mOsm, pH 7.4, all Carl-Roth). The recording chamber was constantly perfused with extracellular solution containing 140 mM NaCl, 2.4 mM KCl, 10 mM HEPES, 2 mM $CaCl_2$, 4 mM $MgCl_2$, and 10 mM glucose (pH adjusted to 7.3 with NaOH, 300 mOsm, all Carl-Roth). For experiments examining postsynaptic receptors (Figure 5 D; Figure 9) we used a Mg^{2+}-free extracellular solution containing 10 μM glycine. Solutions were applied using a fast-flow perfusion system.

For whole-cell voltage clamp recordings, neurons were maintained at -70 mV holding potential. Cells were subjected to 500 ms depolarizations in 10 mV steps from –90 mV to +50 mV to analyze Na^+/Ca^{2+} and K^+ currents.

AP firing patterns and passive membrane properties were recorded in whole-cell current-clamp configuration. Bridge balance was automatically compensated. 300 ms current steps from -40 pA to 120 pA were injected. The resting membrane potentials were analyzed from baseline and the input

resistances were calculated by Ohms law using a current step of -50 pA for 600 ms.

Membranes standing glutamatergic and GABAergic ionotropic receptor function were tested by pulsed application (1 s) of 20 μM kainic acid, 100 μM *N*-Methyl-D-aspartic acid (NMDA) and 5 μM γ-Aminobutyric acid (GABA) (all Tocris). Peak amplitudes from six consecutive sweeps were averaged. The values were normalized to the cell capacitance.

Excitatory postsynaptic currents (EPSCs) were evoked by a 2 ms somatic depolarization from –70 to 0 mV producing an unclamped axonal AP. To determine the size of the RRP, 500 mM sucrose (Sigma Aldrich) solution was applied for 5 s and the resulting transient inward current was integrated (Rosenmund and Stevens 1996). Miniature excitatory postsynaptic currents (mEPSC) were detected using a sliding template function in AxoGraph X (Clements and Bekkers 1997) and false positive events were corrected by using the selective competitive α-amino-3-hydroxy-5-methyl-4-isoxazolepropionic acid (AMPA) receptor antagonist 2,3-Dioxo-6-nitro-1,2,3,4-tetrahydrobenzo[f]quinoxaline-7-sulfonamide (NBQX; 3 μM (Tocris)). The number of vesicles (n_{RRP}) in the RRP was calculated by dividing the charge of the sucrose response (Q_{RRP}) by the average mEPSC charge (Q_{mEPSC}) for each neuron.

$$n_{RRP} = \frac{Q_{RRP}}{\bar{Q}_{mEPSC}} = \frac{\int \left(I_{Sucrose}(t) - I_{steady}\right) dt}{\int \bar{t}_{mEPSC}(t) dt}$$

The P_{VR} was calculated as the ratio of the average EPSC charge (Q_{EPSC}) and the RRP charge.

$$P_{vr}[\%] = \frac{\bar{Q}_{EPSC}}{Q_{RRP}}\ x\ 100 = \frac{\int \bar{I}_{EPSC}(t) dt}{\int \left(Q_{Sucrose}(t) - I_{steady}\right) dt}\ x\ 100$$

The spontaneous release rate was determined by dividing the mEPSC frequency by the number of vesicles in the RRP for each cell. The paired-pulse ratio (PPR) was calculated by applying two stimuli with an inter-stimulus interval (ISI) of 25 ms and dividing the amplitude of the second EPSC by the first EPSC.

For pharmacological studies with 30 μM L-(+)-2-Amino-4-phosphonobutyric acid (L-AP4) (Tocris), 20 μM R-Baclofen (Tocris), 10 μM D-(-)-2-Amino-5-phosphonopentanoic acid (D-AP5) (Tocris), 3 μM NBQX (Tocris) and 1 μM (2S,2'R,3'R)-2-(2',3'-Dicarboxycyclopropyl) glycine (Tocris) baseline EPSC amplitudes were monitored at 0.2 Hz for 30 s without drug application, followed by 30 s in the presence of the drug and another 30 s in the absence of the drug. The degree of EPSC depression or potentiation was determined by dividing the mean EPSC amplitude in the presence of the drug by the overall mean EPSC amplitude before and after drug application in standard extracellular solution of each cell. The degree of EPSC potentiation induced by 1 μM phorbol-12,13-dibutyrate (PDBu) (Tocris) was determined by monitoring EPSC amplitudes at 0.2 Hz for 15 s in standard extracellular solution followed by 30 s under PDBu application. The degree of potentiation was calculated by normalizing the EPSC amplitudes recorded under PDBu application to the mean of EPSC amplitudes recorded in standard extracellular solution.

Western blot

For quantification of Unc13A and protein levels, human iN were lysed 14 days post transduction at 4 °C with lysis buffer (50 mM Tris, pH 8.0, 150 mM NaCl, 0.2 % NP-40, protease inhibitor cocktail complete mini (Roche Diagnostics)). Equal amounts of total protein from the lysates of human iNs transduced with Unc13A-KD or scrambled control virus were separated on SDS polyacrylamide gel and transferred to a nitrocellulose membrane. Membranes were blocked for 1 h with 5 % skim milk in PBS-T and incubated at 4 °C over night with primary antibodies in blocking solution: anti-Munc 13-1

(126103 Synaptic Systems) and anti- β-Tubulin III (T8660 Sigma-Aldrich). Following three 10 min washes with PBS-T the membranes were incubated with the horseradish peroxidase-conjugated secondary antibodies (Jackson ImmunoResearch) in PSB-T for 1h at RT. Detection was performed by using ECL Plus Western Blotting Detection Reagents (GE Healthcare Biosciences) in a Fusion FX7 detection system (Vilber Lourmat). Data were analyzed offline using ImageJ.

To confirm that no Syt1 protein is detectable in the constitutive KO of Syt1, the same protocol as described above was used. The following primary antibodies were used: anti-Syt1 (105011 Synaptic Systems) and anti- β-Tubulin III (T8660 Sigma-Aldrich).

Genetic modification by CRISPR/Cas9

Ribonucleoprotein complex formation and Nucleofection

For the generation of a constitutive iPSC knock out (KO) line for the presynaptic protein Syt1, we used an approach where we delivered a ribonucleoprotein complex (RNP), composed of a short-guided RNA (sgRNA) and the Cas9 Nuclease.

For designing the side specific sgRNAs we used different tools, from Synthego, IDT, and Crispor. In total, we generated 8 different sgRNAs with each platform and had them cross-validated for their on target specificity and off target sites. We decided to attribute a higher value to off target effects than to on target activity. After completion of the analysis, we obtained the four most highly valued sgRNAs (see Figure 12).

To obtain the sgRNA we used the cr:tracrRNA method (trans-activating CRISPR RNA (tracrRNA), CRISPR RNAs (crRNA)). We obtained both components (Alt-R CRISPR-Cas9 crRNA and Alt-R CRISPR-Cas9 tracrRNA) synthesized from IDT. To build the cr:tracrRNA duplex 10 μl of 200 μM crRNA and 10 μl of 200 μM tracrRNA were mixed and incubated for 2 minutes at 94 °C without shaking. The complex was then slowly cooled to RT and stored at -20 °C until use.

One day prior nucleofection two times 500 K cells per nucleofection were seeded. For the formation of the sgRNA/Cas9 complex, 2 µl sgRNA were mixed with 2 µl Cas9 protein (HiFi Cas9 Nuclease V3 from IDT) and incubated for about 20 min at RT. Afterwards, the nucleofection mix was prepared consisting of 82 µl P3 buffer, 18 µl of Supplement 1 (Amaxa Primary Cell Kit P3) and 4 µl of sgRNA/Cas9 complex with 1 µl IDT electroporation enhancer. The iPSCs were then detached using Accutase and centrifuged for 5 min at 300 x g. The supernatant was completely aspirated and iPSCs were resuspended in the nucleofection mix. The sgRNA/Cas9 complex was delivered by nucleofection into the iPSC using an Amaxa 4D Nucleofector (Lonza). The CM-150 program on the Amaxa 4D Nucleofector was used for electroporation. Immediately after nucleofection the transfected iPSCs were seeded into a new 6 well containing StemFlex medium with 2 µM Thiazovivin. Four hours later the complete StemFlex medium in each well was replaced.

CRISPR editing results analysis

The bioinformatics tool ICE (Inference of CRISPR Edits) from Synthego was used to determine the efficiency of the sgRNAs. With the help of this tool, it is possible to obtain results by normal sanger sequencing that come to the quality of next generation sequencing. It only requires a purified PCR product over the sgRNA cleavage site, whose DNA sequence is being compared with an unedited control sequence. DNA was isolated 48 h after sgRNA/Cas9 complex nucleofection of the cells. For DNA isolation the NucleoSpin Tissue KIT (Macherey Nagel) was used according to the manufacturer's instructions, with the modification that only 50 µl buffer BE for eluting the DNA from the column was used. The PCR was performed on the on target side using the primers listed below and the PCR fragment was purified with the QIAquick Gel Extraction Kit (Qiagen). The purified DNA was sent at a concentration of 10 ng/µl for Sanger sequencing using the ready2run sequencing service from LGC Biosearch with the reverse primer of the PCR product (listed below).

The sequencing results were analyzed online in comparison to an unedited control sequence on the Synthego website.

On target PCR for ICE analysis

For the ICE analysis a fragment with a size of 435 bp was produced.

Primers

Primer name	Primer Sequence
Forward 500 bp	GCCCATGAGTTAAAAGGTTTTCCA
Reverse 500 bp	ACCCTGCCAAATGCTTCCAT

PCR Protocol

Component	Concentration	Amount
Forward 500 bp	10 pmol/µl	2.5 µl
Reverse 500 bp	10 pmol/µl	2.5 µl
Phusion GC Buffer	5x	10.0 µl
Phusion DNA Polymerase	2U/µl	0.5 µl
DMSO		2.5 µl
dNTPs	2.5 mM each	2.0 µl
H_2O		29.0 µl
Template DNA		1.0 µl

Cycling Parameters

Step	Temperature	Time
1	98 °C	30 sec
2	98 °C	7 sec
3	65 °C	15 sec
4	72 °C	10 sec
Cycle back to Step 2 35 times		
5	72 °C	10 min
6	12 °C	∞

Generation of single clones

To generate individual clones of the selected KO Syt-1 and thus a new clonal cell line, the cells were nucleoporated with sgRNA #1 as described above. This sgRNA was chosen as it proved to be the one with the highest efficiency in the previously conducted preliminary tests. After nucleoporation, the cells were placed in StemFlex medium containing CloneR (STEMCELL Technologies). 24 h later, a limited dilution was performed with one cell per 200 µl of medium. A total of 192 wells were plated in 48 well plates with 200 µl per each well. The medium was changed every 24 h. CloneR supplement was included in the medium for the first 72 h. Afterwards StemFlex medium according to the manufactures protocol was used. During the next three to four weeks, the cells were continuously expanded, until two confluent wells of each original colony were obtained in a 12-well plate. One well was cryopreserved in Bambanker (NIPPON Genetics) and stored at -80 °C until further use. The other well was used to isolate DNA as described above and used for the confirmation of the correct genetic modification.

Control for OFF-target effects, clonality and karyotyping

Amplicon next generation sequencing was used (Amplicon-EZ, Genewiz) to check individual iPSC clones for their clonality. For this a purified PCR fragment (See above for the procedure. Primers for the PCR fragment are listed below) of 500 ng (20 ng/µl) was used. The analysis of the sequencing data generated from the Illumina platform was performed directly by the sequencing company (Genewiz).

After clonality was confirmed the clones were analyzed for their karyograms (in collaboration with the BIH core facility Stemcells and the Human Genetics Practice of the Charité Berlin). Freshly thawed iPSC clones were passaged 5 times and sent for diagnostic analysis at the Institute of Medical and Human Genetics of the Charité Berlin.

Off-target effects off sgRNA were assessed by normal sanger sequencing and Cas-OFFinder (CRISPR RGEN Tools, http://www.rgenome.net/cas-offinder) with a mismatch number of 2 or less.

Amplicon NGS and off target PCR

For the NGS analysis a fragment of 199 bp was produced.

Primers

Primer name	**Primer Sequence**
Forward NGS	GCCCATGAGTTAAAAGGTTTTCCA
Reverse NGS	TTCCCTCCTTTTTCCTTTCCC

PCR Protocol

Component	**Concentration**	**Amount**
Forward 500 bp	10 pmol/µl	2.5 µl
Reverse 500 bp	10 pmol/µl	2.5 µl
Phusion GC Buffer	5x	10.0 µl
Phusion DNA Polymerase	2U/µl	0.5 µl
DMSO		2.5 µl
dNTPs	2.5 mM each	2.0 µl
H_2O		29.0 µl
Template DNA		1.0 µl

Cycling Parameters

Step	**Temperature**	**Time**
1	98 °C	30 sec
2	98 °C	7 sec
3	62 °C	15 sec
4	72 °C	10 sec
Cycle back to Step 2 35 times		
5	72 °C	10 min
6	12 °C	∞

Off target PCR conditions

The following primer pairs were used to detect off target effects and created fragments of about 200 bp.

Primers

Primer name	Primer Sequence
Forward Chr1	TTCCTCCTGGATACTCCCGTGGCT
Reverse Chr1	AAGCAGGACACCCATCCCTGC
Forward Chr4	CAGATTTGAGATGTAGTCCTGTG
Reverse Chr4	CTAATCTTACGAAAATGGAACACTG
Forward Chr5	GACATGACAACTAAATGCAATGTAC
Reverse Chr5	ATGTTCATATCCTAACTCCCAGAGTC
Forward Chr9	GCTACTGCCTTGATTCACAATGC
Reverse Chr9	ATTAGGATGATGGAATCATAGGCC
Forward Chr12	ATGGCTGTGTTGGTGATGAGG
Reverse Chr12	GTAATATCCAGTGTCTATCTTCC
Forward Chr14	GGCTCTGCTCACTCCACAAGTC
Reverse Chr14	TTACAAGTGTAGAGTCACCTCTG

PCR Protocol

Component	Concentration	Amount
Forward	10 pmol/µl	2.5 µl
Reverse	10 pmol/µl	2.5 µl
Phusion GC Buffer	5x	10.0 µl
Phusion DNA Polymerase	2U/µl	0.5 µl
DMSO		2.5 µl
dNTPs	2.5 mM each	2.0 µl
H_2O		29.0 µl
Template DNA		1.0 µl

Cycling Parameters

Step	Temperature	Time
1	98 °C	3 min
2	98 °C	30 sec
3	58 °C for 4 and 12 62 °C for 1,5,9 and 14	20 sec
4	72 °C	20 sec
	Cycle back to Step 2 30 times	
5	72 °C	5 min
6	12 °C	∞

Statistic

Data were collected from 2–9 independent human iN autaptic cultures to account for putative culture to culture variability. Independent human iNs cultures were generated by an individual induction process from each human iPSC line for each replicate. For electrophysiological experiments, an equal number of recordings per experimental group in each replicate culture were obtained.

Statistical significance was determined by using the two-tailed Mann Whitney test for unpaired data at the given significance level (*$p < 0.05$, **$p < 0.01$, ***$p < 0.001$) using GraphPad Prism 7.

Chapter III

Results

Results

Autaptic culture of human induced neurons

The properties of iPSC lines generated by different methodologies can vary extensively (Bardy, van den Hurk et al. 2016). To ensure that INs obtained from iPSCs could generate autaptic human iNs, cultures independently of the origin or the methodology used for the iPSC generation, we used two independent iPSC lines provided by the Berlin Institute of Health Core Facility Stem Cells (Berlin, Germany): the iPSC line BIHi001-A derived from human foreskin fibroblasts using Sendai virus vectors and the iPSC line BIHi004-A derived from human fibroblasts using episomal vectors.

In initial experiments, we differentiated iNs from iPSCs by overexpression of NGN2 to obtain a pure glutamatergic neuron population for the production of autaptic cultures using the protocol described by Zhang and colleagues (Zhang, Pak et al. 2013). Human iNs mass cultures were then dissociated at day 4 post induction (DPI) and plated directly onto mouse-derived astrocytic microislands at a density of 4 K cells per 6 Well to allow them to grow independently on single islands. Using this approach, after 6 weeks in autaptic culture human iNs showed very low survival, not suitable for electrophysiological or morphological characterization required to validate this protocol. Shorter cultivation times on the autaptic islands led to a lack of measurable synaptic transmission. The survival rate of neurons until the time of measurable synaptic activity was so low, far below one percent, that even an increase of the initially seeded human iNs would not have led to a sufficient result. However, the few measured synaptic responses from the surviving human iNs did not differ in their physiological or morphological parameters from those in the new protocol developed in the following study. It should be noted, though, that due to the small sample number (n) no statistical statement can be made. The low survival rate of the human autaptic iNs can be explained by the observation that astrocytic microislands rarely remained healthy for longer than 4 weeks, limiting the overall time *in vitro* of the autaptic iNs. However, it led us to hypothesize that the development of the human iNs may

require a period of significant cell-to-cell contacts with other neurons in order to mature sufficiently like it is seen in normal mass cultures.

We therefore used the differentiation protocol by Zhang and colleagues to obtain human iNs and created a different two phased protocol to produce the autaptic human iNs cultures. In the first phase we allowed the human iNs to develop within the network of mass culture. To support neuronal survival on day 4 we added mouse astrocytes on top of the human iNs as described by Zhang and colleagues. Despite the fact that human iNs grew extensive neurites during the first phase, we were able to efficiently dissociate them for replating. In the second phase, human iNs were plated on astrocytic microislands, subsequently cultured and allowed to grow for another 14 to 21 days before they were used for morphological and functional characterization (Figure 3 A).

We observed that the duration of phase I played an important role to successfully obtain electrophysiological responses in the autaptic human iNs. To determine the optimal time point needed for the human iNs in phase I, we performed a timeline experiment, in which we kept the human iNs 14, 35 and 60 days in the first phase before we replated them onto the microislands. Following another 14 to 21 days onto microislands, we performed whole-cell patch-clamp recordings in order to examine the passive and active membrane properties of autaptic human iNs (Figure 3 B). Regardless of the time of human iNs in phase I all autaptic human iNs developed voltage-dependent sodium and potassium currents and robust AP firing. In contrast, only 44 % of the autaptic human iNs exhibited spontaneous release (mEPSC) at 14 and 35 days in phase I. In line, only 14.3 % of the autaptic iNs being 14 days in phase I, showed evoked NT release (EPSC) and 32 % at 35 days. For human iNs being 60 days in the first phase, an average of 80 % of the cells showed both spontaneous and evoked NT release (Figure 3 B). Longer periods in the first phase did not result in a significant difference compared with the 60 day time point (data not shown). Therefore, we defined 60 days in phase I as the necessary time point when synaptic transmission can be reliably measured to replate human iNs for the generation of fully functional human autaptic iNs,

which can be examined after additional 14-21 days on the astrocytic microislands.

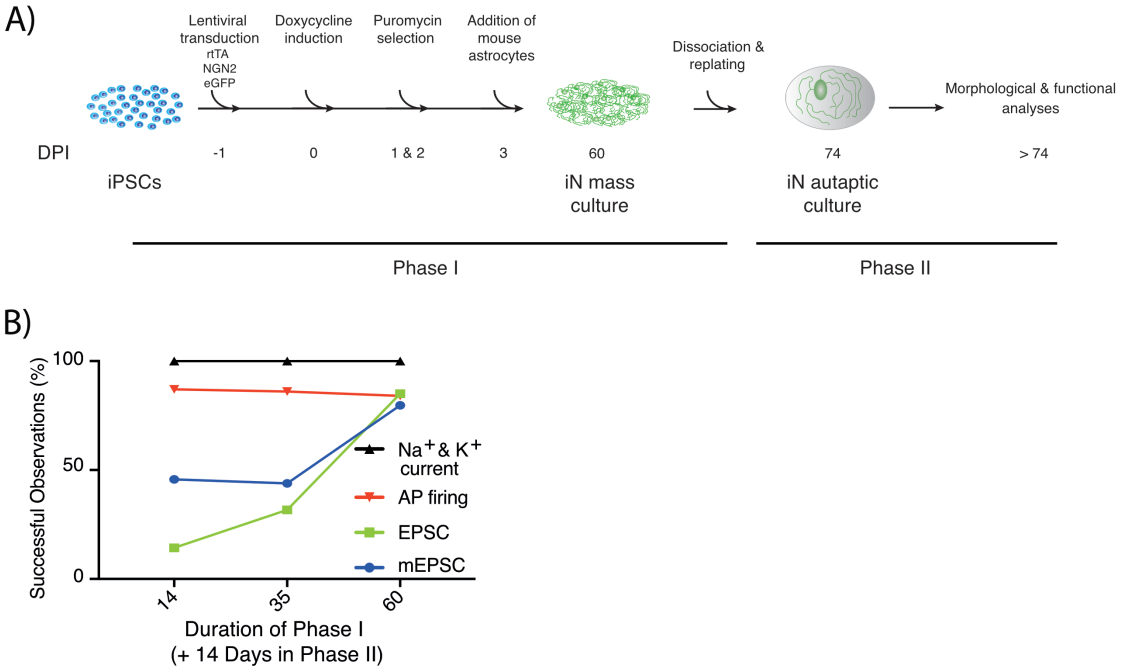

Figure 3: Human neurons in autaptic culture

A) *Schematic diagram of the autaptic culture protocol for human iNs. IPSCs were plated and infected with NGN2, rtTA and eGFP on day –1, followed by application of doxycycline to start Ngn2 expression and puromycin selection on day 0 to 3. Mouse astrocytes were added on day 3 and co-cultured for 60 days, followed by dissociation with Accutase and replating onto astrocytic microislands. Single autaptic iNs were analysed after additional 14-21 days on microislands feeder cultures.* ***B)*** *Quantification of electrophysiological recordings of autaptic iNs replated on microislands after 14, 35 or 60 DPI in the mass-culture phase I, followed by another 14-21 days of cultivation on microislands in phase II.*

Morphology of human iNs in autaptic cultures

We first assessed whether human autaptic iNs generated with our new protocol possessed the same general morphological characteristics as glutamatergic autaptic neurons obtained from murine hippocampi. We determined the following morphological parameters in the autaptic human iNs, length of dendrites and axons and the number of synapses, by applying immunocytochemical methods. Quantitative analysis of MAP2 -positive neurites showed that the dendritic trees were shorter, compared to murine hippocampal neurons (Sampathkumar, Wu et al. 2016), with mean lengths of 377 ± 83 μm and 253 ± 35 μm for iNs derived for the BIHi001- and BIHi004-iPSC lines, respectively (Figure 4 A). Axonal length, determined by the mixture of monoclonal antibodies that react against complex network proteins of axons (SMI 312), showed that the human iNs axons' reached 4.5 ± 0.6 mm and 3.0 ± 0.3 mm in BIHi001- and BIHi004- derived iNs, respectively (Figure 4 A). Interestingly, these axons are 50 - 250% longer than those of primary mouse hippocampal neurons in autaptic culture (Sampathkumar, Wu et al. 2016).

After determining the dendritic and axonal lengths, we quantified the synapse number and density of the autaptic human iNs by counting synaptophysin-positive puncta distributed along the MAP2-positive dendrites (Figure 4 B). Synapse densities were 26 ± 3 and 42 ± 3 per 100 μm in the human iNs derived from BIHi001- and BIHi004- iPSC lines, respectively, while the total synapse number for the human iNs derived from BIHi001- and BIHi004- iPSC lines were 98 and 106 synapses per cell, respectively. Synapse densities were comparable to those of rodent neurons in autaptic culture (Sampathkumar, Wu et al. 2016).

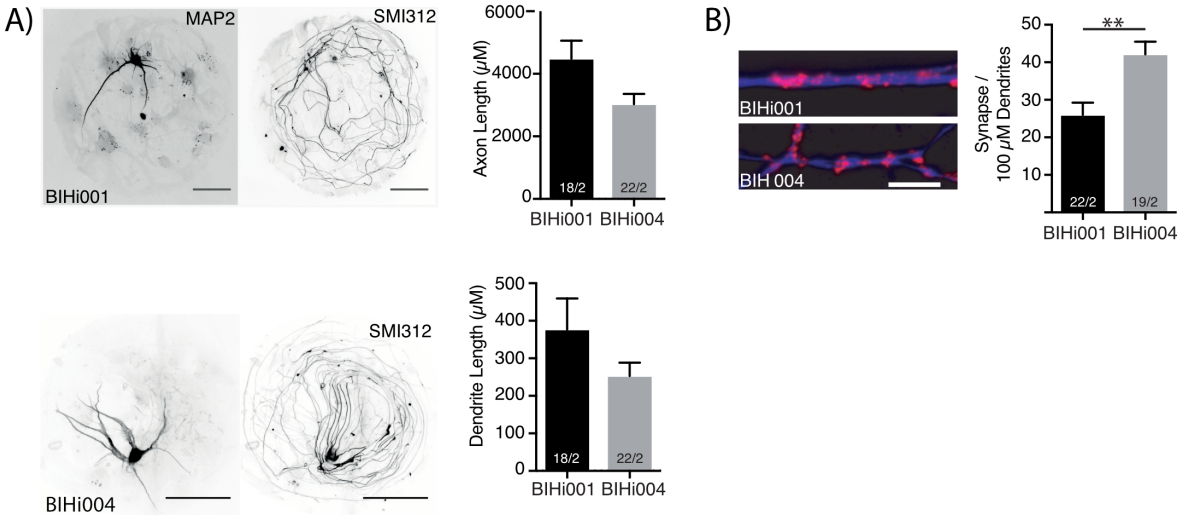

Figure 4: Morphological analysis of human induced neurons in autaptic culture

A) *Representative images and quantification of total axonal and dendritic lengths of human autaptic iNs. Dendrites were identified by MAP-2 staining and axons were stained with SMI-312. Images in each row belong to the same iN lines. Scale bars: 50 µm.* ***B)*** *Example images and quantification of synapse density in human autaptic iNs. Synapses were identified by Synaptophysin labelling. Only Synaptophysin punctae (red) on top of MAP-2 staining (blue) were counted. Scale bars: 5 µm. The numbers of human INs and independent cultures analysed are shown within the bars. Data are expressed as mean ± SEM.*

Passive membrane properties and ion channel characteristics

After assessing morphological features, we wanted to examine functional properties of the autaptic human iNs. We used current-clamp experiments to demonstrate the ability to fire AP and showed that upon injection of 20 pA iNs started to show robust AP firing. The number of APs increased constantly with an increase in injected current. The two cell lines exhibited no significant differences. (Figure 5).

We next performed whole-cell current and voltage-clamp recordings in order to examine their passive and active membrane properties (Figure 5). Both human autaptic iNs derived from BIHi001- or BIHi004-iPSC lines had similar resting membrane potentials of approximately -55 mV. Additionally, both lines presented same input resistances of approximately 375 MΩ and showed comparable membrane capacitances around 30 pF (Figure 5 A). Furthermore, all autaptic iNs recorded showed voltage-dependent sodium and potassium currents (Figure 5 B, also see Figure 6 A).

We quantified excitatory (Glutamate) and inhibitory (GABA) NT receptor functionality in our human iNs by exogenous application of the respective agonists (Figure 5 D). Application of kainic acid (20 μM), an agonist of the kainite-class ionotropic glutamate receptors, elicited a mean current density of approximately 10 pA/pF, indicating the presence of functional glutamate receptor. In contrast, application of the aminoacidic derivative NMDA (100 μM) yielded negligible currents, indicating poor expression of NMDA-type glutamate receptors. However, direct application of the GABA aminoacid (5 μM) led to robust responses in all iNs tested (Figure 5 D) proving the existence of functional GABA ionotropic receptors ($GABA_A$). While the two human autaptic iNs derived from the different lines varied in mean current density (BIHi001, 92.9 ± 12.6 pA/pF and BIHi004, 62.9 ± 11.9 pA/pF), these results indicate the presence of AMPA and GABA receptors in human autaptic iNs derived from both iPSC lines.

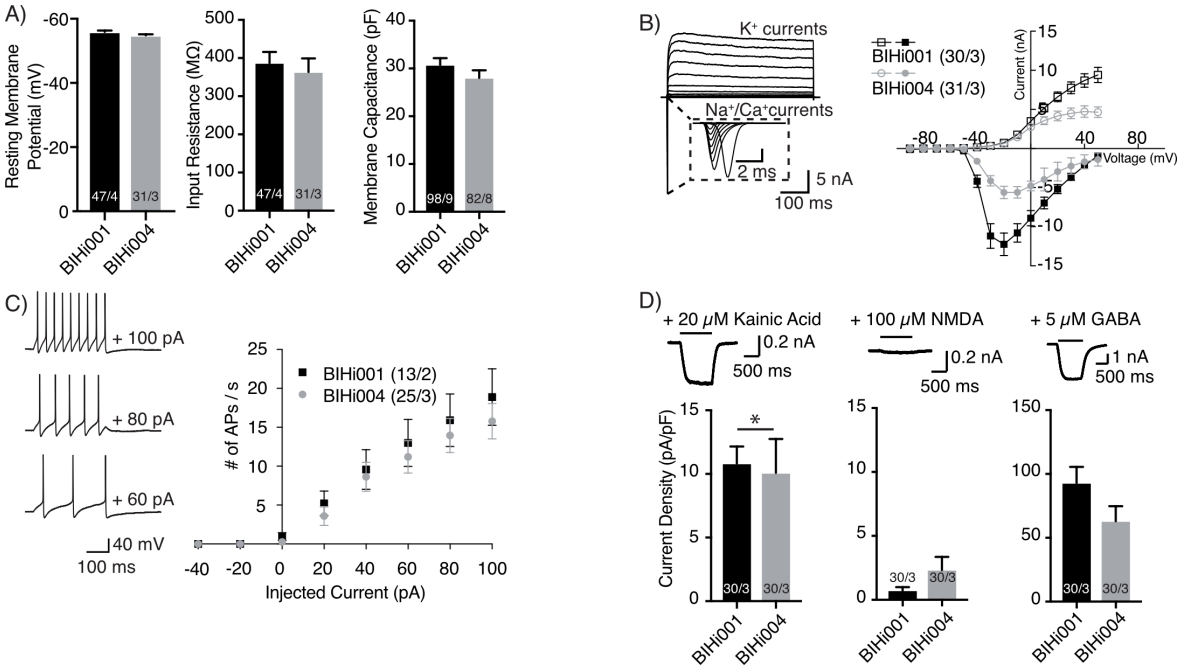

Figure 5: Passive membrane properties and ion channel characteristics of iNs grown in autaptic culture

A) *Average resting membrane potential, input resistance and membrane capacitance of human autaptic iNs.* ***B)*** *Representative whole-cell voltage-clamp traces (left) and quantitative analysis of Na^+/Ca^{2+} and K^+-currents (right) measured with whole-cell voltage-clamp.* ***C)*** *Representative traces (left) and quantitative analysis of the number of APs per second elicited by current injections in current-clamp recordings (right).* ***D)*** *Quantification of postsynaptic currents evoked by application of either 20 µM kainic acid (left), 100 µM NMDA (middle) or 5 µM GABA (right) in the presence of 10 µM glycine and in the absence of Mg^{2+}. The numbers of neurons and independent cultures analysed are shown within the bars. Data are expressed as mean ± SEM.*

Neurotransmission in autaptic human iNs

Since we observed robust synapse formation and functional postsynaptic receptors for AMPA, we next assessed functional properties of autaptic human iN synapses by whole-cell voltage-clamp recordings. Upon a 2 ms somatic depolarization to induce an evoked AP, a large majority of the human iNs (85 %) responded with a rapidly decaying synaptic inward current, demonstrating the high efficiency of the culture protocol (60 days phase I + 14-21 phase II) for generating functional and mature autaptic human iNs. The synaptic responses recorded confirm the existence of neurotransmitter release and the functionality of the postsynaptic receptors. (Figure 6 A). The postsynaptic inward currents were robust with mean amplitudes of 1.1 ± 0.2 nA and 1.0 ± 0.1 nA for BIHi001- and BIHi004- derived human iNs, respectively (Figure 6 B). Application of the AMPA receptor antagonist NBQX quantitatively blocked the postsynaptic currents, confirming the glutamatergic phenotype of the release and that most of the postsynaptic current was carried by the AMPA receptors. On a side note, the time between the AP induction and postsynaptic response was more variable (data not shown) than in murine autaptic cultures, which we attributed to more extensive axonal outgrowth in the human neurons (Figure 4 B).

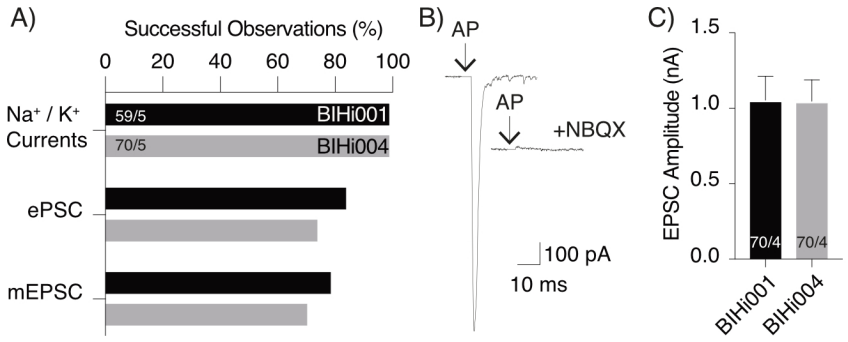

Figure 6 Action potential-evoked neurotransmitter release

A) *Fraction of neurons which showed membrane voltage-dependent K^+ and Na^+/Ca^{2+} currents, EPSC and mEPSC in autaptic human iN cells.* ***B)*** *Representative traces of AP-evoked EPSCs recorded in the absence or presence of the AMPA receptor antagonist NBQX.* ***C)*** *Mean AP-evoked EPSC amplitudes of iNs induced from BIHi001- and BIHi004-iPSCs. AP artefacts were blanked and are indicated by black arrows. The numbers of neurons and independent cultures analysed are shown within the bars. Data are expressed as mean ± SEM.*

One of the major advantages of the single cell autaptic culture system is that it allows for the quantification of the RRP, which is a product of the number of fusion-competent vesicles in all synapses of a given neuron. One way by which the RRP can be assessed is by the application of a pulse (5 seconds) of a hypertonic sucrose solution onto the neurons using a fast-flow perfusion system (Rosenmund and Stevens 1996). The sucrose application results in a postsynaptic inward current that represent the release from all fusion competent synaptic vesicles (RRP). The charge of the sucrose-evoked current can be quantified by integrating this current transient (Figure 7 A) and thus estimating the RRP. The mean RRP charges were 50 ± 10 pC and 67 ± 11 pC for BIHi001- and BIHi004- derived iNs, respectively.

In the absence of stimulation, we recorded spontaneous neurotransmitter release indicated by mEPSCs (Figure 7 B). The mean mEPSC amplitude was significantly smaller in BIHi004- compared to BIHi001-derived human iNs (Figure 7 C; BIHi001: 39.7 ± 2.4 pA; BIHi004: 30.4 ± 2.8 pA, Mann-Whitney U test, p = 0.0024). However, spontaneous release frequencies were non-significant around 2 Hz for both iN lines

(Figure 7 B). Using the average mEPSC charge and the RRP charge, we calculated the total number of SVs in the RRP. BIHi001-derived human iNs had an average of 618 ± 97 vesicles in the RRP (Figure 7 D). In contrast, for BIHi004-derived iNs the average number of vesicles in the RRP was 869 ± 113. We could estimate the number of SVs in the RRP per synapse from the average number of synapses per cell. This resulted in an average of 6.2 fusion-competent SVs per synapse for BIHi001 and 8.2 fusion-competent SVs per synapse for BIHi004.

Knowing the RRP and the action potential-evoked EPSC charges we determined the fusion efficiency of individual fusion-competent vesicles by calculating the (P_{VR}). P_{VR} is the likelihood that a given synaptic vesicle is released in response to an action potential. We found that the P_{VR} was 14.2 ± 2.3 % and 11.1 ± 2.1 % in BIHi001- and BIHi004-derived iNs, respectively (Figure 7 E).

We also calculated the spontaneous release rates of individual fusion-competent vesicles by normalizing the mEPSC frequency (Figure 7 B) to the RRP size (Figure 7 E). Human iNs had a surprisingly high spontaneous release rate compared with mouse hippocampal neurons (Arancillo, Min et al. 2013) but comparable to thalamical neurons (Albright, Weston et al. 2007), where 0.8 ± 0.1 % and 0.5 ± 0.2 % of the RRP is turned over within a second in BIHi001- and BIHi004- derived iNs, respectively (Figure 7 F).

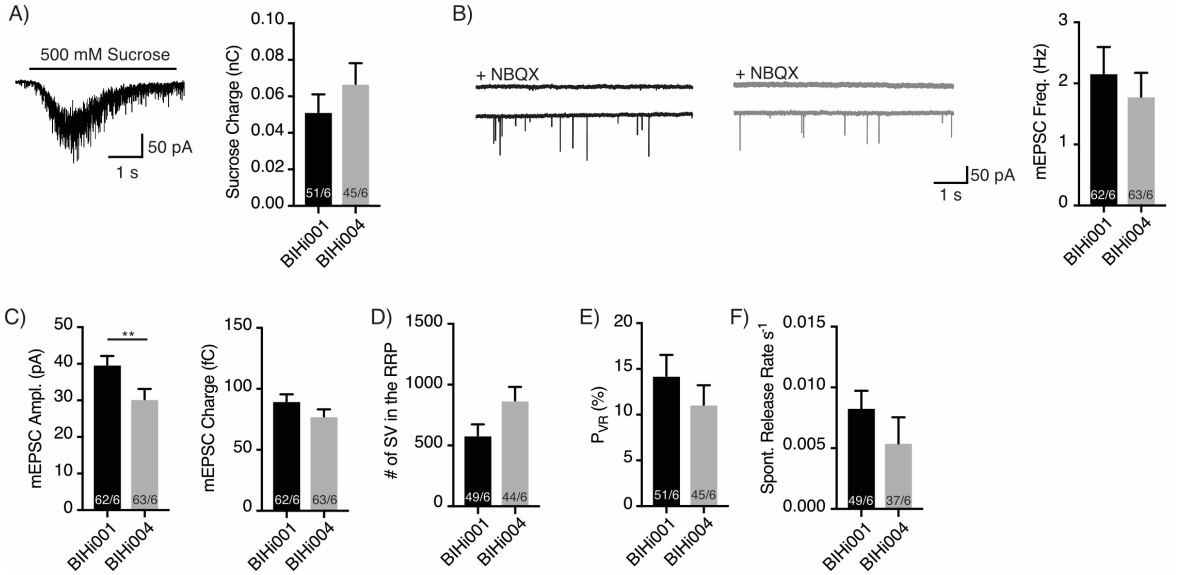

Figure 7 Pool size and spontaneous neurotransmitter release

A) *Exemplary trace of the synaptic response of an autaptic iN elicited by 500 mM hypertonic sucrose solution (left) and average size of the RRP charges (right* ***B)*** *Exemplary mEPSCs recorded from autaptic iNs in the absence or presence of NBQX (left) and mean mEPSC frequencies of human autaptic iNs derived from the BIHi001- and BIHi004 iPSC lines (right).* ***C)*** *Mean amplitudes and charges of mEPSCs.* ***D & E)*** *Number of SVs in the RRP (D) and mean* P_{VR} *(E).* ***F)*** *Spontaneous release rate of human autaptic iNs. The numbers of human iNs and independent cultures analysed are shown within the bars. Data are expressed as mean ± SEM.*

Another way to determine the release probability is to look for facilitation or depression of the postsynaptic currents under a series of multiple stimulations. For this purpose we used a 40 Hz paired pulse stimulation protocol (25 ms ISI, Figure 8 A) and a protocol with a train of 50 AP at a frequency of 10 Hz (10 Hz 50 AP, Figure 8 B). In both cases we could see a strong depression, which correlated with the high vesicular release probability found.

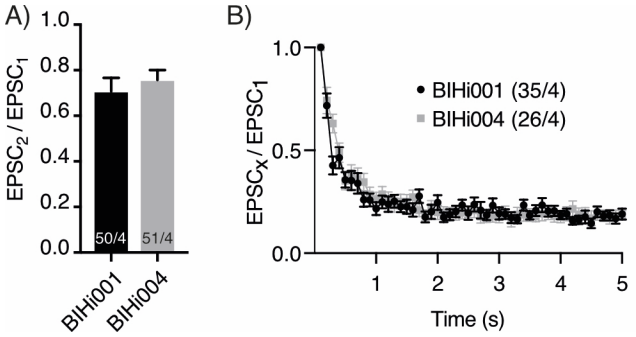

Figure 8 Short term plasticity

A) *Average paired-pulse ratios (PPR) calculated from two EPSCs with an ISI of 25 ms.* ***B)*** *Normalized EPSC amplitudes during a 10 Hz train stimulation. The numbers of human iNs and independent cultures analysed are shown within the bars. Data are expressed as mean ± SEM.*

Postsynaptic responses are mediated by AMPA receptors

We next examined the glutamatergic receptor composition and assessed the relative contribution of each receptor type to synaptic transmission at the human iN postsynapse. We utilized specific antagonists for AMPA (NBQX; 3 μM) and NMDA receptors (D-AP5; 10 μM). The results showed slight differences between the iN lines. While BIHi001-derived iNs indicated no evidence of NMDA receptor - mediated synaptic transmission, BIHi004-derived iNs showed around 5 % contribution of NMDA receptors to EPSC amplitudes (Figure 9). These data demonstrated that autaptic human iNs contains a robust expression of AMPA receptor but a general deficiency of NMDA receptor expression, consistent with our results obtained from exogenous application of AMPA and NMDA receptor agonists (Figure 5 D).

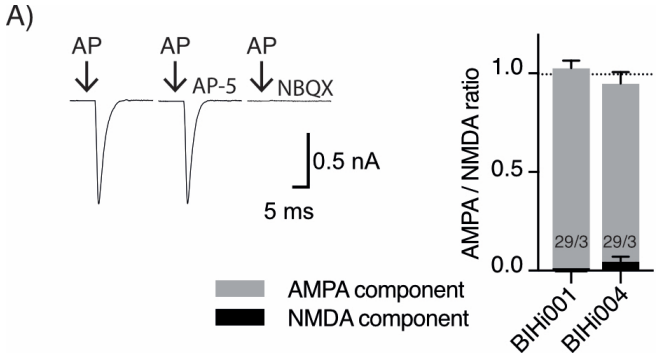

Figure 9: AMPA/NMDA ratio in iN

Components of the EPSCs mediated by AMPA and NMDA receptors. AP artefacts were blanked and are indicated by black arrows. The numbers of neurons and independent cultures analysed are shown within the bars. Data are expressed as mean ± SEM.

Modulation of glutamate release by metabotropic receptors and phorbol esters

In a next step, we assessed how release from human glutamatergic synapses is modulated by well-known modifiers of release. First, we applied the $GABA_B$ agonist Baclofen (20 μM), which is known to robustly inhibit release of excitatory glutamatergic synapses (Scanziani, Capogna et al. 1992). Indeed, we found that Baclofen rapidly and reversibly reduced EPSC amplitudes by 69 % and 77 % in BIHi001- and BIHi004- derived iNs, respectively (Figure 10 A). These results demonstrate that the human iNs express presynaptic $GABA_B$ receptors and efficiently couple them to the release apparatus.

We also examined metabotropic glutamate receptor (mGluR) modulators and noticed that 1μM DCG-IV, an agonist for type II mGluRs, significantly reduced Ca^{2+} evoked synaptic transmission in human autaptic iNs (9.2 % in BIHi001-derived iNs; 7.4 % in BIHi004-derived iNs; Figure 10 B). Nevertheless, only BIHi004-derived iNs responded to activation of type III mGluRs by the agonist L-AP4 (30 μM) with a small but significant reduction of EPSC amplitudes by 12 % (Figure 10 C).

Finally, we examined the synaptic response potentiation by phorbol esters, which are known to modulators of vesicle fusogenicity through activation of the Munc13 family of proteins (Rhee, Li et al. 2005, Basu, Betz et al. 2007). Application of 1 μM of the phorbol ester PDBu rapidly increased the evoked responses, plateauing at 123 % and 142 % in BIHi001- and BIHi004-derived iNs, respectively (Figure 10 D). The overall degree of potentiation was modest, consistent with the high initial release probability (Figure 7) (Basu, Betz et al. 2007, Shin, Lu et al. 2010).

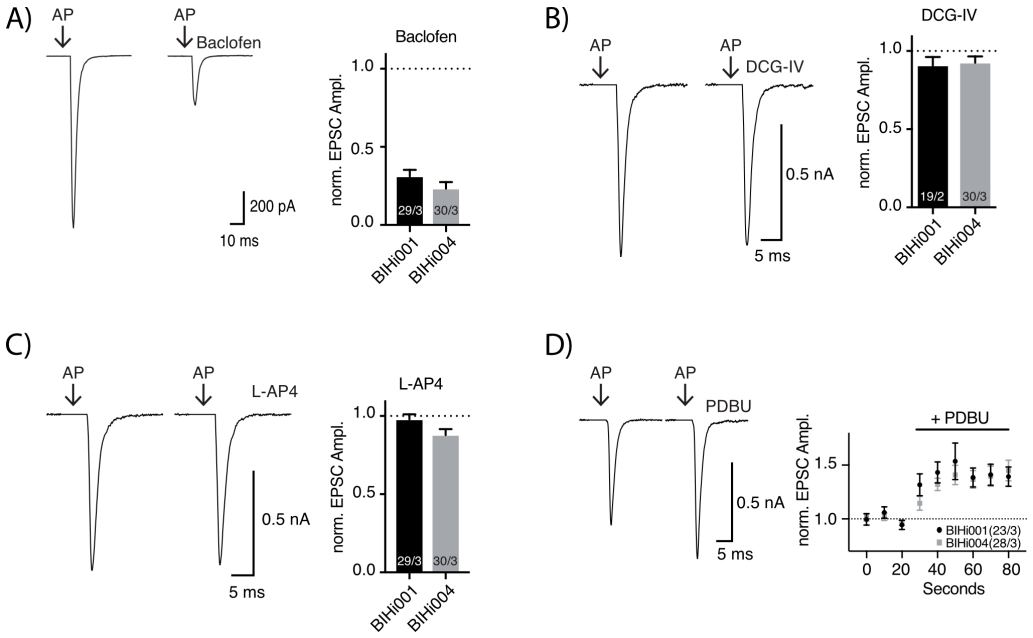

Figure 10: Modulation of glutamate release by metabotropic receptors and phorbol esters

A) *Comparison of EPSC amplitudes with and without Baclofen, DCG-IV* ***(B)*** *and L-AP4* ***(C)****.* ***D)*** *EPSC potentiation by application of PDBu. AP artefacts were blanked and are indicated by black arrows. The numbers of neurons and independent cultures analysed are shown within the bars. Data are expressed as mean ± standard error of mean (SEM).*

Unc13A KD abolishes RRP of vesicles and NT release

One of our main goals behind the development of the autaptic human iN model system was to reliably study the neurotransmission process in human neurons. To validate the reliability and reproducibility of our system, we also aimed to investigate this process in the absence of one of the essential elements of the NT release machinery, the docking/priming factor Unc13. For this reason, we genetically modified the human iNs after replating using a shRNA-based KD assay for Unc13A. Lentiviral transduction of Unc13A-specific shRNA in iNs led to a nearly complete loss of Unc13A protein levels assayed by western blot of lysates of 14 DIV mass-cultured human INs replated after 60 days in phase I (Figure 11 A). Knocking-down Unc13A in autaptic human iNs resulted in a complete absent of evoked NT release (Figure 11 B). Furthermore, in these human iNs no measurable RRP could be detected by application of hypertonic sucrose solution (Figure 11 C). These results validate our model and demonstrate, that human Unc13A has an indispensable role in the priming step of the NT release in the human INs, as it has been observed in mouse loss-of-function models for Munc13-1 (Varoqueaux, Sigler et al. 2002).

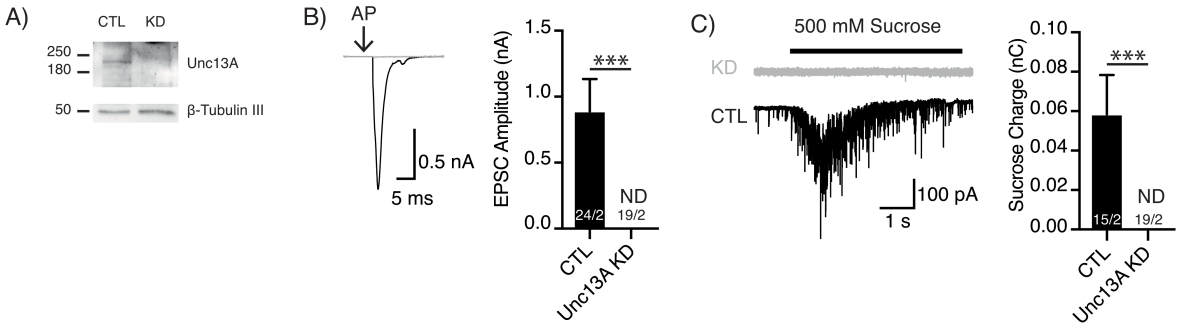

Figure 11: Loss of function by knocking down Unc13A in BIHi001.

A) *Immunoblot of Unc13A protein levels of mass culture human iNs transduced with a shRNA against Unc13A or a control construct. Signal at 200 kDa corresponds to Unc13A, and the signal at 50 kDa to β-Tubulin. Western blot images have been cropped for better illustration.* ***B)*** *Exemplary traces of AP-evoked EPSCs (left) and average EPSC amplitudes (right) in Unc13A KD and control (CTL) conditions of BIHi001 cells.* ***C)*** *Exemplary traces of currents evoked by 500 mM hypertonic sucrose solution (left) and average sizes of the RRP charges (right). (ND, not detectable). AP artefacts were blanked and are indicated by arrows. The numbers of human iNs and independent cultures analysed are shown within the bars. Data are expressed as mean ± SEM.*

Generation of a constitutive KO for Synaptotagmin 1 by CRISPR/Cas9

IPSC have a high potential to represent models of pathophysiological diseases of the CNS and have the power to better reflect the human phenotype compared to transgenic animal models. With the help of CRISPR/Cas9, genetic defects can be imitated in healthy donor cells or repaired in diseased lines. This will serve us after the generation of autaptic human INs, together with a lentiviral rescue approach, as an ideal tool for *in vitro* disease modeling to study the effects in the human neurotransmission process of mutations in genes encoding synaptic proteins.

Synaptotagmin 1 (Syt1) has been described as the main Ca^{2+} sensor for neurotransmitter release and a Syt1 KO mice have been well characterized as a model to study synchronous release (Fernandez-Chacon, Konigstorfer et al. 2001, Chang, Trimbuch et al. 2018). Additionally, known genetic mutations in human Syt1 gene have been associated with the neurodevelopmental disorder Baker Gordon syndrome, making it a very interesting model protein to test in our iNs (Baker, Gordon et al. 2015, Baker, Gordon et al. 2018). To study possible defects in neurotransmission in the Baker Gordon syndrome we attempted to produced autaptic human iN cultures generated from a homozygous KO iPSC line for the presynaptic protein Syt1.

For the generation of a constitutive KO for Syt1 in human iPSC we decided to produce a frame shift in exon 5, which translates for the beginning of the transmembrane domain, using CRISPR/Cas9. This is predicted to result in an early stop codon that disrupts the translation of Syt1 and causes the elimination of Syt1. The four highest ranked sgRNAs, as predicted by bioinformatic tools (see material and methods), were used for the generation of the constitutive KO (Figure 12 A). After a further validation of the efficiency for the production of insertions or deletions to the DNA we decided to continue with sgRNA#1 as it scored highest in the prediction to generated a Syt1 KO (Figure 12 B). Using sgRNA#1, we targeted exon 5 in our BIHi005 iPSC line and isolated a total of 102 individual clones. After another round of sequencing

over the on-target region we selected 6 clones (clones 2, 7 ,30, 31, 40 and 59). We confirmed that the 6 clones had stop codons at different positions of exon 5 and that the stop codons were always at the beginning of the area corresponding to vesicular transmembrane domain, except for clone 2. The stop codons were generated either by insertion of 2 bases in case of clone 7 or by deletions of 1 to 25 bases for the other clones (Figure 12 C).

A)

sgRNA	Guide sequence
1	ATTGCAATTAAGGCCCACGG
2	GCTATTGCAATTAAGGCCCA
3	GTTTCTTTCAGTGCCACCGT
4	TGTTTCTTTCAGTGCCACCG

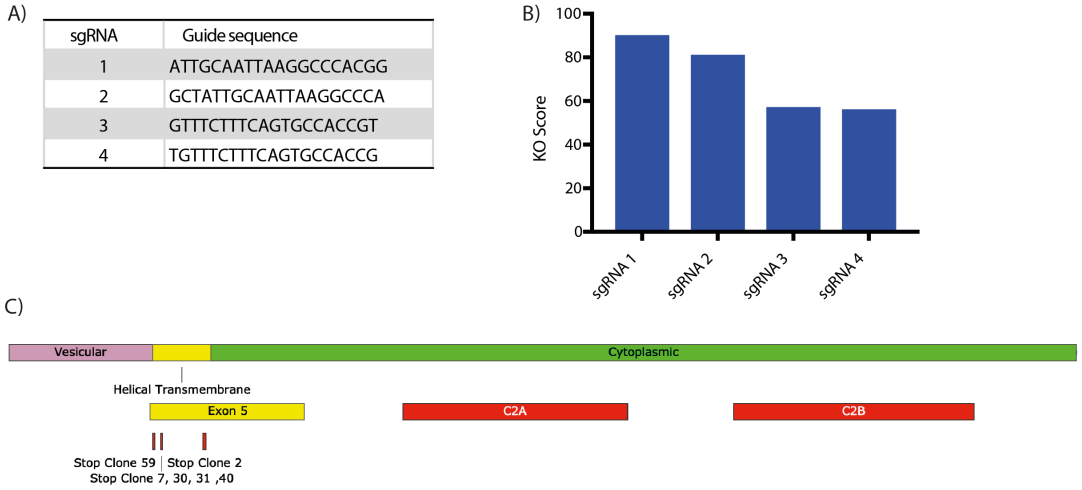

Figure 12 Guide RNA design and evaluation

A) *Table showing the 4 top scored sgRNA used for Nucleofection.* ***B)*** *Summary of KO score validation by bioinformatic analysis (ICE from Sythego).* ***C)*** *Scheme of Syt1 Protein and the location of exon 5. Red bars indicating insertion of stop codon from the different clones after clonal selection.*

The 6 clones were further examined for their clonality using next generation sequencing. A PCR fragment spanning a 250 base pair area over the edited site was sequenced using the Illumina Platform. After filtering, a total of about 60000 reads were obtained and compared to the unedited wild type (WT) sequence. The clonality was confirmed for the top 6 clones (Figure 13 A). To narrow down the number, we decided to continue with clone number 7 and 59. In clone number 7, the stop codon occurred at the amino acid positions 61 by an insertion of 2 bases and in clone number 59 the stop codon occurred at position 58 due to a deletion of 25 bases. This means that for both clones the stop codons are located in the transmembrane region of the protein and

the remaining fragment length is about 6 kDa. Karyograms of the 2 clones were obtained and revealed no abnormalities regarding the chromosome set or the morphology of the individual chromosomes indicating no additional chromosomal abnormalities in the clones (Figure 13 B). Predicted potential off target regions of our sgRNA#1 were checked by Sanger sequencing clone 7 and 59. Analysis of the sequences spanning off target regions on chromosome 1, 4, 5, 9, 12 and 14 (for details see material and methods) could not detect any changes in the DNA.

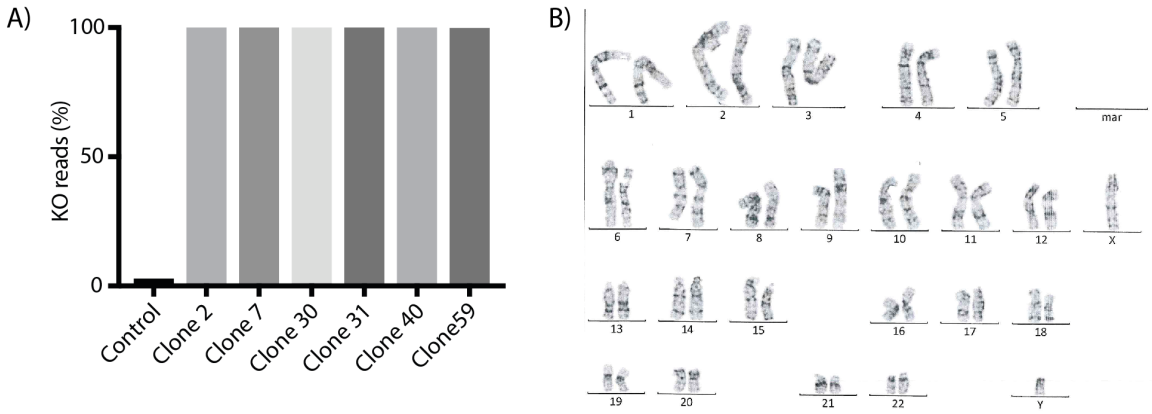

Figure 13 Quality control of generated clones

A) *Results of amplicon sequencing validating clonality of all 6 clones in comparison to WT.*

B) *Example karyogram of a diploid male chromosome set from clone 7.*

Synaptic transmission in human Syt1 deficient neurons

After we established the human INs Syt1 KO, we used the culture protocol developed above to perform western blots from mass cultures and electrophysiological measurements in autaptic human iNs.

To ensure that all observed effects were caused by the loss of Syt1 we used two different clones namely clone 7 and 58. A western blot using an antibody against the c terminus of Syt1 showed the complete loss of the protein in mass cultured neurons of both Syt1 KO clones. Employing electrophysiological recordings, we found a dramatic loss of evoked AP neurotransmitter release. This was reflected by the reduction of the EPSC amplitude by 90 % for clone 7 and 87 % for clone 59. The reduction of 40 % for both clones of the EPSC charge integrated for 1 s (Figure 14). This data was consistent with the loss of asynchronous release observations detected in the Syt1 KO mouse model. However, the reduction of the EPSC charge was smaller than reported from autaptic cultures from the KO mice (Xue, Ma et al. 2008).

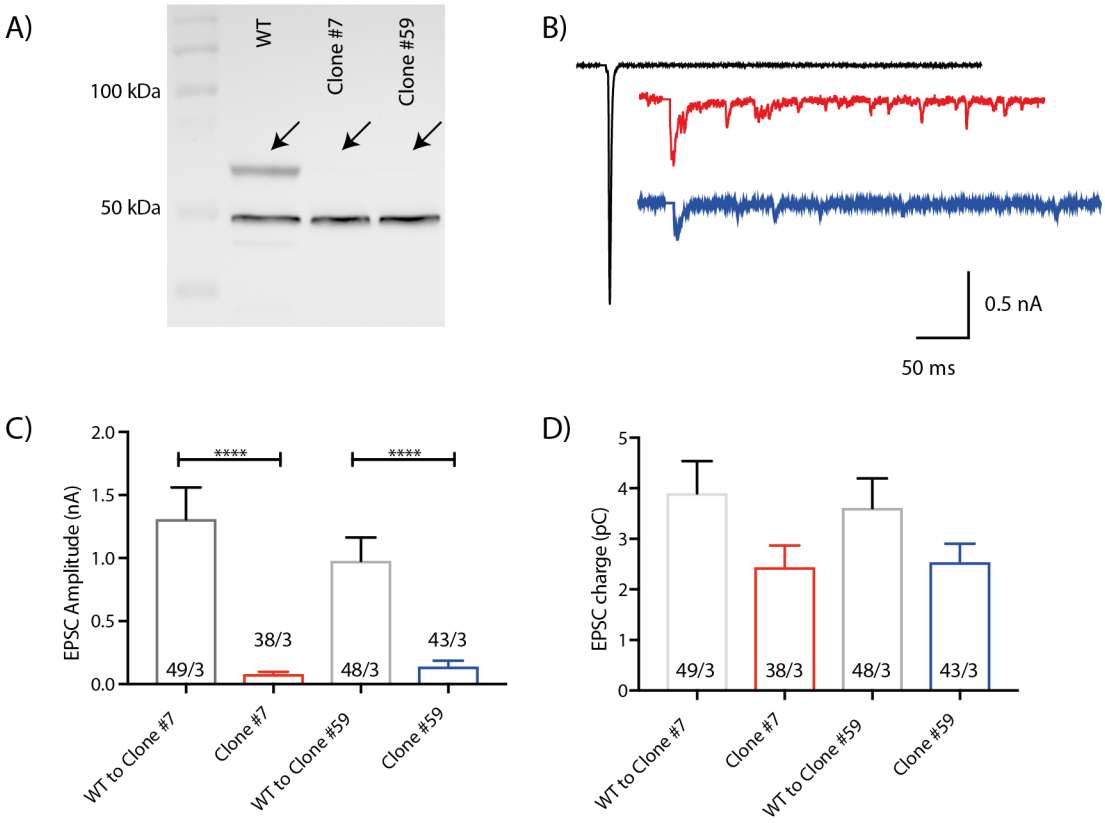

Figure 14 Evoked responses of Syt1 KO neurons

A) *Western blot from mass cultured human iNs showing the loss of Syt1 in clone #7 and clone #59 (arrow, expected band at 65 kDa).* ***B)*** *Representative traces of AP-evoked EPSCs from WT (black) or Syt1 KO (red and blue) human INs.* ***C & D)*** *Mean AP-evoked EPSC amplitudes (B) and charges (C) of iNs from both KO clones in comparison to their corresponding WT CTL cell line. The number of neurons and independent cultures analysed are shown within the bars. Data are expressed as mean ± SEM.*

Application of 500 mM sucrose to measure the RRP independent of calcium influx revealed, that the total RRP was not significantly reduced in the Syt KO iNs clones. However, the release probability of AP evoked vesicle fusion was reduced by approximately 50 % (Figure 15 A, B) whereas the mouse model showed a stronger reduction of about 80 % (Xue, Ma et al. 2008). The reduced P_{VR} was also reflected when we applied short term plasticity protocols. When human iNs were stimulated with two depolarizing pulses with an ISI of 25 ms, both Syt1 KO human iNs clones show a stronger facilitation of the second EPSC amplitude, approximately 3 times compared to the WT iNs that cause a depression of the second EPSC of about 20 %. (Figure 15 C). This data correlate with the lower vesicular release probability of 11.4 % for clone 7 and 11.8 % for clone 59 compared to the WT with 25.8 %. Under sustained stimulation at synapses with low vesicular release probability, calcium accumulates at the release sites, increasing the release probability of the vesicles that facilitates the following evoked responses. This was observed in both clones upon stimulation at 10 Hz for 5 seconds (Figure 15 D).

Using unstimulated traces and looking for spontaneous NT release we could not find any significant differences neither for the frequency nor for the charge or amplitude (Figure 15 E).

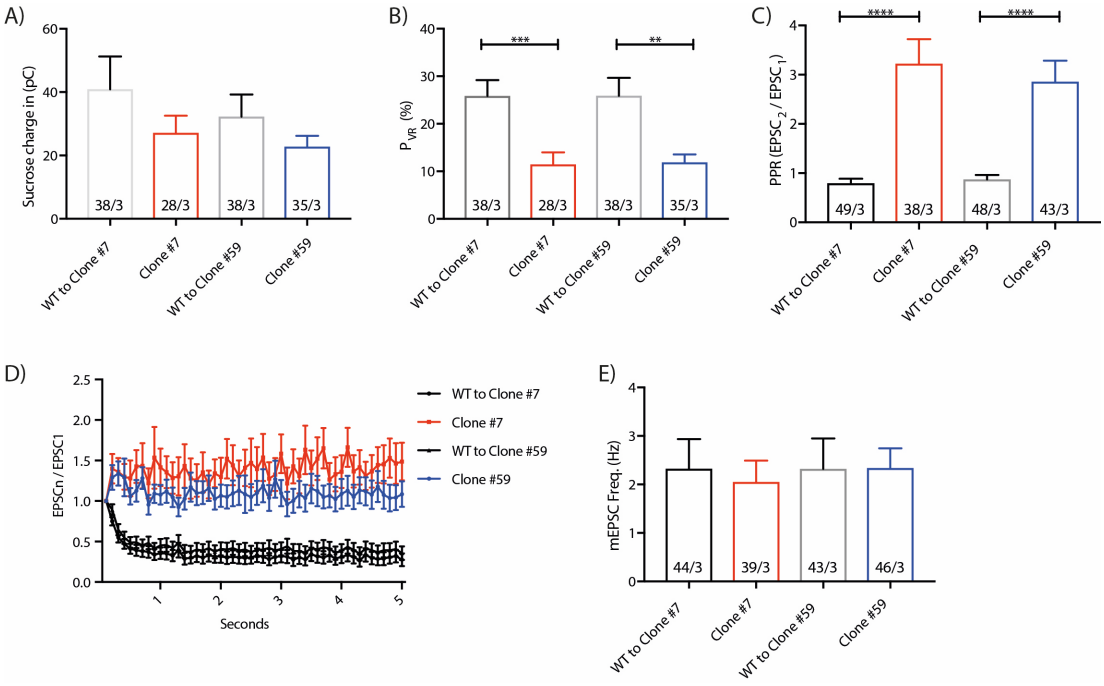

Figure 15 Release probability of Syt1 KO neurons

A & B) *Number of SVs in the RRP (A) and mean P_{VR} (B).* ***C)*** *Average paired-pulse ratios (PPR) calculated from two EPSCs with an ISI of 25 ms.* ***D)*** *Normalized EPSC amplitudes during a 10 Hz train stimulation.* ***E)*** *Mean mEPSC frequencies of Syt1 KO neurons in comparison to their WT CTL. The numbers of neurons and independent cultures analysed are shown within the bars. Data are expressed as mean ± SEM.*

Even though we used two individual Syt1 KO clones, there is still the possibility that the observed phenotypes are due to off target mutations. To rule out that possibility, we used lentiviral transduction to express the full-length cDNA of Syt1 to see if we could restore the Syt1 protein levels and obtain the WT phenotype. Since we could not depict any major differences between clone number 7 and clone number 59, we decided to perform these experiments only with clone number 7. Lentiviral transduction to reintroduced the protein was performed 24 h after splitting the cells on autaptic feeder islands, followed by a further cultivation for 14 to 21 days before performing the electrophysiological recordings.

The evoked response was rescued to 70 % compared to the WT CTL with no significant difference between this groups (Figure 16 A, B). The other two main phenotypes observed in the Syt1 KO were the reduced P_{VR} and increased STP. Short-term plasticity for the KO showed a strong facilitation in the PPR and the 10 Hz stimulation over 5 seconds. With the reintroduction of the full length cDNA we see the same depression in 10 Hz and PPR as for the corresponding WT control (Figure 16 C, E). Additionally, P_{vr} was restored to the level of WT, by reintroduction of Syt1 (Figure 16 D). These results confirm that our Syt1 KO is both specific and functional. In addition, it demonstrates for the first time the usability of the CRISPR/Cas9 in human autaptic iNs.

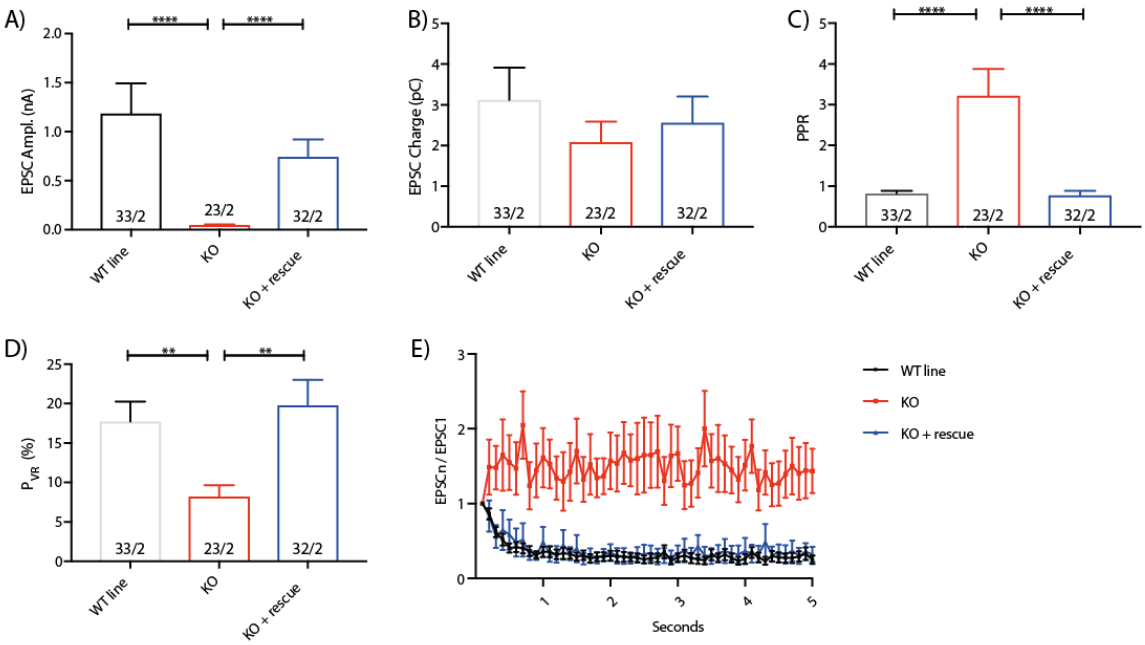

Figure 16 Syt1 KO can be rescued by reintroducing human cDNA

A) *Mean AP-evoked EPSC amplitudes showing significant reduction for the KO and through lentiviral overexpression, the restoration of WT level.* ***B)*** *Mean AP-evoked EPSC charge showing a trend for a reduction for the KO and no difference for the rescue construct* ***C)*** *Average paired-pulse ratios (PPR) calculated from two EPSCs with an ISI of 25 ms* ***D & E)*** *Mean P_{VR} showing the lower release probability for the KO which correlate with the facilitation during the 10 Hz train (E) and PPR (C) and through lentiviral overexpression, the restoration of WT phenotypes for those parameters. The numbers of neurons and independent cultures analysed are shown within the bars. Data are expressed as mean ± SEM.*

Chapter IV

Discussion

Discussion

In this study, we established the first protocol for the autaptic culture of human iPSC-derived neurons. We developed a two-phase protocol that was validated on different iPSC cell lines. This way we could reliably demonstrate that our method robustly generates mature human neurons, that are capable to grow in isolation on astrocytic microislands and form functional synapses onto themselves. The morphological and functional properties of these human induced neurons and their synapses are accessible to highly quantitative analysis. Hence, our approach allows future analysis of drug- or genetically induced phenotypes with higher precision whilst offering more sophisticated methods of analysis than what is currently possible with culture methods. Additionally, we successfully modified gene expression using two different approaches in the autaptic human iN leading to major changes in the recorded synaptic properties. In a first step, we used a shRNA based knockdown of the well-described Unc13 protein during the autaptic phase. In a second step, we developed a constitutive KO cell line for Syt1 using CRISPR/Cas9.

Autaptic iNs show robust synapse formation

To establish autaptic cultures of human iNs we had to overcome two major difficulties: the limited life time of the astrocytic microislands (Emperador Melero et al. 2017), and the fact that human iNs do not like to exist in isolation. While optimizing our culture protocol we noticed that we could split mass cultured human iNs after 60 days, thereby circumventing both obstacles. Therefore, we argue that the modified culturing procedure, of splitting it up into two phases, still represents a precise method for the analysis of synapse formation, maintenance and density.

In comparison to already known protocols for neurons differentiated from embryonic stem cells in mass culture, we found that the autaptic iNs had passive membrane properties which were comparable to previous studies (Zhang, Pak et al. 2013, Pak, Danko et al. 2015, Patzke, Han et al. 2015, Patzke, Acuna et al. 2016, Yi, Danko et al. 2016, Gunhanlar, Shpak et al. 2018)

and can also be transferred to those from mouse models (Mangan and Kapur 2004). Although our culturing procedure generates neurons with relatively shorter dendrites than classical culturing methods, the density of synapses formed is comparable to other experimental approaches (Chang, Trimbuch et al. 2014, Sampathkumar, Wu et al. 2016, Wu, Lee et al. 2016). We do not think this is specific for human iNs but rather caused by the replating or culturing procedure because mass-cultured iNs do have longer dendrites (Patzke, Han et al. 2015, Patzke, Acuna et al. 2016, Gunhanlar, Shpak et al. 2018). In contrast, the axonal outgrowth appears much more resilient to replating, as axon lengths were comparable to mass-cultured human iNs (Patzke, Acuna et al. 2016) and were 50 - 250 % longer than those of primary mouse hippocampal neurons in autaptic culture (Sampathkumar, Wu et al. 2016). The synapse densities were comparable to those of autaptic rodent neurons (Chang, Trimbuch et al. 2014, Sampathkumar, Wu et al. 2016). However, due to the shortened dendrites, the total synapse numbers were reduced accordingly.

Quantitative determination of synaptic input and output function, and determination of synaptic efficacy

Using the presented technique, the alterations in important synaptic parameters, such as release probability, can now be analyzed and compared in a more comprehensive quantitative manner. The functional properties of the autaptic iNs were overall consistent with the mass-cultured iNs described by Zhang and colleagues, which also showed a lack of NMDA receptor expression (Zhang, Pak et al. 2013). However, our recorded synaptic responses were much larger than those measured in mass culture (Zhang, Pak et al. 2013, Pak, Danko et al. 2015, Patzke, Han et al. 2015, Yi, Danko et al. 2016). Depending on the presynaptic stimulation technique (e.g. paired recordings, field stimulation) the responses in mass culture only reflect a small and highly variable fraction of the synaptic input onto the recorded postsynaptic neuron. For example, using local field stimulation, the fraction of

synapses stimulated is strongly dependent on the geometry of the electrical field generated by the stimulator. Furthermore, the input derives from multiple presynaptic neurons. On the other hand, the autaptic culture system has the unique advantage that inputs are monosynaptic and originate all from the same neuron, explaining our observed larger synaptic responses compared to published mass culture recordings. Additionally, the autaptic culture systems allows for quantitative assessment of the total synaptic input and output of a given neuron with a single AP stimulation. Still, when we compare our synaptic responses with those recently published in human autapses from other laboratories, our responses were up to 5 times smaller (Meijer, Rehbach et al. 2019, Rhee, Shaib et al. 2019). This can be explained by the fact that all synaptic responses with EPSC amplitudes smaller than 500 pA were removed from the statistics in Meijer et. al (Meijer, Rehbach et al. 2019). These strict exclusion criteria make it difficult to study models in which the EPSC amplitude is smaller than in WT due to the phenotype. Therefore, we decided to include all data points in our analysis.

Combined functional and morphological analysis in the autaptic human iNs is particularly suitable for describing the properties of individual human synapses in greater detail. We observed, for example, that the number of easily releasable SVs per synapse ranged from 5 to 10 vesicles per nerve ending, a value similar to that reported in rodent hippocampal neurons (Schikorski and Stevens 1997, Murthy, Schikorski et al. 2001). Computation of release probability and spontaneous release rates indicated that human iN vesicles display a rather high fusogenicity, reminiscent of high release probability glutamatergic neurons in the sensory pathways, such as thalamic (Albright, Weston et al. 2007, Weston, Nehring et al. 2011) and layer 4 cortical neurons (Feldmeyer 2012). High vesicle fusogenicity is also consistent with the moderate potentiation by PDBu application (Figure 10) (Basu, Betz et al. 2007, Shin, Lu et al. 2010). The mechanism for the rather high fusogenicity is unknown, but may relate to the expression of the VGLUT subtype 2 (Zhang, Pak et al. 2013), which is known to be associated with intrinsically higher release probability (Weston, Nehring et al. 2011).

Assessment of modulation of synaptic responses by exogenous modifiers of synaptic transmission

Presynaptic metabotropic receptors and their associated second messenger systems play an important role in proper neuronal and brain function (Huang and Thathiah 2015). Modulation of NT release by the activation of presynaptic metabotropic receptors is a common target in drug development and treatment of several neuropsychiatric disorders (Miyamoto, Miyake et al. 2012, Aleman, Lincoln et al. 2017, Bruno, Caraci et al. 2017). The identification of the particular set of metabotropic receptors expressed by human iNs is therefore particularly important. At the same time, assessment of the modulation of NT release by second messenger systems requires reliable quantification of evoked synaptic responses, which is the major advantage of the autaptic cell culture system. Using our autaptic culture system for human iNs, we showed for the first time, that synaptic transmission of these neurons is reliably modulated by $GABA_B$ and metabotropic glutamate receptors.

Modification of gene expression in individual neurons, enabling loss of function and mutational studies in the human biological background

Over the last few years analysis of the human genome has revealed numerous genetic mutations related to pathophysiological changes in neuronal development and brain function. Understanding the basic mechanisms of these mutations has been studied exclusively in animal models, especially in mice (Hofker, Fu et al. 2014). Cutting-edge developments in genetic methods and stem cell programming for the first-time can provide direct access to human genetically modified neurons, offering a potential alternative to animal models. Therefore, we wanted to test if we could recapitulate the loss of function phenotype of UNC13A in rodent neurons to the human homologue of Munc13-1 with shRNA based KD in our iNs.

We demonstrated that using shRNA-based KD assays during replating is sufficient to generate *loss-of-function* models for synaptic proteins. The KD of Unc13A recapitulated the complete disruption of synaptic NT release in *Munc13-1/2* double KO rodent neurons (Varoqueaux, Sigler et al. 2002). Hence, our described two-phase protocol for autaptic iNs is especially flexible for protein structure-function experiments and modelling of human diseases. With the KD assay it is sufficient to keep one or two lines of wildtype iNs during the mass-culture phase, which can then be used for lentiviral transduction of shRNA, to study different protein functions during the autaptic culturing phase.

First, we demonstrated the ability to acutely knock out proteins with shRNA, we then went a step further. Neurons generated from patient-derived human iPSCs hold great promises for the detection of synaptopathies, which are thought to be the basis of many human neuropsychiatric and neurological diseases. In conjunction with *in situ* genome editing, it allows for a simpler identification and analysis of developmental, morphological and/or functional aspects of putative pathophysiological mechanisms (Chao, Zoghbi et al. 2007, Priller, Dewachter et al. 2007, Chao, Chen et al. 2010, Weston, Chen et al. 2014, Sampathkumar, Wu et al. 2016, Lipstein, Verhoeven-Duif et al. 2017). Since the genetic background of patient derived human iPSC is not fully understood, we used CRISPR/Cas9 to generate a constitutive KO which can be used to study patient-related mutations by lentiviral overexpression of the mutated protein of choice. We decided to use Syt1, a well-studied protein in the mouse model (Brose, Petrenko et al. 1992, Geppert, Goda et al. 1994, Xue, Ma et al. 2008, Chang, Trimbuch et al. 2018), which is associated with neuronal developmental disorders (Baker, Gordon et al. 2015, Baker, Gordon et al. 2018, Bradberry, Courtney et al. 2020). For this purpose, we targeted exon 5 of Syt1 and introduced a premature stop codon, leading to the loss of the protein, by means of RNP complex and non-homologous end joining. The advantage of this method is that the introduction of the synthetic RNA and the Cas9 protein only leads to minimal OFF targets effects because the whole RNP complex is degraded after a few hours (Kim, Kim et al. 2014).

The examination of the KO of Syt1 showed that the synchronous NT release was impaired in these neurons. This can be explained by the fact that the vesicular protein Syt1 is a Ca^{2+}-binding protein, which is responsible for fast and synchronous fusion, as shown in the mouse model (Brose, Petrenko et al. 1992, Geppert, Goda et al. 1994, Fernandez-Chacon, Konigstorfer et al. 2001). However, a reduction of the SV pool is only minimal. This indicates that the number of fusion competent vesicles is not reduced, which could be shown in the mouse model by both electrophysiological measurements and electron microscopic images (Geppert, Goda et al. 1994, Chang, Trimbuch et al. 2018). From this it can be concluded that the role of Syt1 as a calcium sensor alone has an effect on the probability of release. Syt1 KO neurons show a lower release probability and strong facilitation in STP. The reintroduction of the cDNA of Syt1 using lentivirus was able to reverse all previously observed phenotypes. Thus, we could show that the observed phenotype is solely due to the loss of the protein. This makes it possible to perform structure function analyses in the human autaptic culture model in the future, making it a powerful tool for studying disease models.

Conclusion

The availability of iPSC enables us for the first time to obtain human neurons from a cell culture approach and thus allows us not only to replace laboratory animals but also to study human diseases directly in a human model. Until now, this has not been possible due to the scarcity of human brain material and the lack of functional protocols for the quantitative analysis of human neuronal phenotypes. The major challenge was that cultured human neurons develop more slowly than mouse neurons. This is especially true for the maturation of synaptic transmission, which is an indicator of neural maturity and is a core factor of neuronal function. While mouse synapses mature in vitro within 2 weeks, human neurons need 6 weeks or more (Bardy, van den Hurk et al. 2016). For that reason, so far only mass cultured human neurons have been used to study human synapse function (Zhang, Pak et al. 2013,

Yang, Chanda et al. 2017). The depth of analysis and quantification of synaptic properties and parameters is limited due to the complex network formed in mass culture. The better alternative is the single autaptic culture in which individual neurons grow isolated on micro-islands of astrocytes and form synapses exclusively with themselves. We have successfully established a protocol that makes it possible to obtain autaptic cultures from human iNs. With the presented technique the alterations in important synaptic parameters, such as release probability, can now be more comprehensibly analyzed and compared in a much more quantitative manner. Additionally, the autaptic cell culture constitutes a system in which function and morphology are much better integrated.

While our analysis identified variations in some of the morphological and functional properties of the two iN lines, the overall differences were rather small, emphasizing the robustness and stability of our system. Moreover, the differences we encountered may have arisen from genetic and epigenetic variations within the iPSC lines (Liang and Zhang 2013). However, when using the technology developed in this study to model synaptic disorders, one should keep in mind to ensure using the correct CTL group. We show that a KO of Syt1 generated by CRISPR/Cas9 could be completely rescued by the reintroduction of the full-length protein. However, the question is whether the differences in physiological parameters in the initial characterization indicates the need for isogenic pairs. This question will need further examination. Currently, our analysis of the Syt1 KO cell line shows that it is a fully adequate replacement for the animal model. The proof of principle of this system now opens up new ways to study patient derived mutations and their effects on synaptic transmission. Furthermore, by generating knock in and deletion / insertions mutations using the CRISPR/Cas9 system new insights can be gained both in homozygote and heterozygous backgrounds. During the generation of a knew cell line a mixed population of homozygous and heterozygous clones is obtained, which makes the direct comparison of homozygous and heterozygous phenotypes in the same genetic background possible.

In principle, the described electrophysiological, pharmacological and immunocytochemical analyses of neuronal morphology and function can be extended to a two-neuron microcircuit system. This would allow the study of interactions between different cell types as well as mutant and wildtype cells (Liu, Chapman et al. 2013, Chang, Trimbuch et al. 2014, Wierda and Sorensen 2014, Sampathkumar, Wu et al. 2016). The human autaptic culture also represents a powerful method for the analysis of synapse formation and maintenance and synapse density. In addition, this technique can be combined with other commonly used methods, such as calcium and vesicle pH dynamics imaging (Herman, Ackermann et al. 2014) or electron microscopy. This would allow for further analysis of the SV cycle. Finally, combining the electrophysiological functional analysis of disease-related phenotypes with Patch-Seq approach (Cadwell, Palasantza et al. 2015, Bardy, van den Hurk et al. 2016) will aid the identification of molecular pathways that underlie the observed phenotypes.

Summary

Human iNs derived from iPSCs hold great potential for modeling human neurological disorders and understanding their underlying causes. Until now, functional analysis of human iNs has been performed in conventional mass culture systems. Though useful for studying iN phenotypes, conventional cell culture lacks the ability to quantitatively characterize developmental and synaptic phenotypes at the individual cell level. That can be achieved with a more specialized cell culture system, such as the single neuron autaptic culture.

Here, we developed a two-step protocol to generate autaptic cultures of iPSC-derived iNs using two independent iPSC lines and a neuronal induction protocol based on NGN2 expression. In the first experiments we show that our method efficiently generates mature, autaptic iNs with normal synapse densities. In these human iNs we were able to measure robust spontaneous and AP driven glutamatergic synaptic transmission. Furthermore, the sensitivity of synaptic responses to modulation by agonists of metabotropic receptors as well as potentiation by acute phorbol ester application.

In the second part of this work we performed an application-based validation of the autaptic human iNs from human iPSCs. This allowed us to demonstrate the reliability of our cell culture system of human iNs as a replacement for animal models. As a proof of principle, we first used an acute shRNA based knocked down of UNC 13-A. Therefore, we added the knock down construct during the second phase of the newly developed protocol, which was only 14 days prior the experimental analysis in the autaptic cultures. We showed that the loss of UNC13A leads to a disruption of NT release. As a second approach we generated a human stem cell line deficient for Synaptotagmin 1, combined with the lentiviral reintroduction of Syt1. Using this approach, we tested the sensitivity of our protocol for the generation of human neural microcultures through the investigation of synaptic transmission in comparison to the known effect in mouse models. We were able to show that the phenotype caused by the loss of the Syt1 protein was similar to the mouse

model and could be rescued by the reintroduction of the Syt1 protein. These results prove the reliability as a model system for further experiments.

We propose that the human iN autaptic culture system provides a versatile platform allowing for quantitative and integrative assessment of morphophysiological parameters underlying human synaptic transmission. Moreover, it can yield crucial information about developmental and functional synaptopathies, which are thought to cause many neuropsychiatric and neurological disorders.

Zusammenfassung

Humane iNs, die von iPSCs abgeleitet sind, besitzen ein großes Potenzial für die Modellierung neurologischer Störungen von Patienten und der Untersuchung der zugrunde liegenden Ursachen. Bisher wurde die funktionelle Analyse humaner iNs in konventionellen Massenkultursystemen durchgeführt. Obwohl sie für die Untersuchung von iN-Phänotypen geeignet sind, fehlt es konventionellen Zellkulturen an der notwendigen Leistungsfähigkeit zur quantitativen Charakterisierung von Entwicklungs- und synaptischen Phänotypen auf der Ebene einzelner Zellen. Dies kann nur durch ein spezialisiertes Zellkultursystem erreicht werden, wie z.B. die autaptische Einzelneuronen-Kultur.

Wir entwickelten dazu ein Zwei-Phasen-Protokoll zur Erzeugung autaptischer Kulturen von iPSC-derivierten iNs, unter Verwendung zweier unabhängiger iPSC-Linien und eines neuronalen Induktionsprotokolls, das auf der Expression von NGN2 basiert. In den ersten Experimenten zeigten wir, dass unsere Methode auf effiziente Weise voll entwickelte, autaptische iNs mit normaler Synapsendichte erzeugt. In diesen autaptischen humanen iNs konnten wir eine robuste spontane und AP-induzierte glutamaterge synaptische Übertragung messen. Darüber hinaus wurde die Sensitivität synaptischer Antworten auf die Modulation durch Agonisten von metabotropen Rezeptoren, sowie die Potenzierung durch akute Phorbolesterapplikation gemessen.

Im zweiten Teil dieser Arbeit führten wir eine anwendungsbasierte Validierung der autaptischen humanen Neuronen aus humanen iPSCs durch. Damit konnten wir die Zuverlässigkeit unseres Zellkultursystems aus humanen Neuronen als Ersatz für Tiermodelle nachweisen. Als „Proof-of-Principle“ verwendeten wir zunächst einen akuten shRNA-basierten „knocked down“ von UNC 13A. Wir fügten das Knockdown-Konstrukt in der zweiten Phase des neu entwickelten Protokolls hinzu, d.h. nur 14 Tage vor der experimentellen Analyse in den autaptischen Kulturen. Wir zeigten, dass der Verlust von UNC13A zu einer Unterbrechung der NT-Freisetzung führt. Als zweiten Ansatz

generierten wir eine humane Stammzelllinie, die für Syt1 defizient ist, kombiniert mit der lentiviralen Reinduzierung von Syt1. Mit diesem Ansatz testeten wir die Sensitivität unseres Protokolls für die Erzeugung humaner neuronaler autaptischer Kulturen durch die Untersuchung der synaptischen Übertragung im Vergleich zu dem bekannten Effekt in Mausmodellen. Wir konnten zeigen, dass der durch den Verlust des Syt1-Proteins verursachte Phänotyp dem Mausmodell ähnlich war und durch die erneute Einbringung des Syt1-Proteins wiederhergestellt werden konnte. Diese Ergebnisse belegen die Zuverlässigkeit als Modellsystem für weitere Experimente.

Wir sind der Meinung, dass das humane autaptische iN-Kultursystem eine vielseitige Plattform bietet, die eine quantitative und qualitative Bewertung der morphologischen und physiologischen Parameter ermöglicht, die der humanen synaptischen Übertragung zugrunde liegen. Darüber hinaus kann es entscheidende Informationen über entwicklungsbiologische und funktionell bedingte Synaptopathien liefern, von denen man annimmt, dass sie viele neuropsychiatrische und neurologische Störungen verursachen.

References

Alabi, A. A. and R. W. Tsien (2013). "Perspectives on kiss-and-run: role in exocytosis, endocytosis, and neurotransmission." Annu Rev Physiol **75**: 393-422.

Albright, M. J., M. C. Weston, M. Inan, C. Rosenmund and M. C. Crair (2007). "Increased thalamocortical synaptic response and decreased layer IV innervation in GAP-43 knockout mice." J Neurophysiol **98**(3): 1610-1625.

Aleman, A., T. M. Lincoln, R. Bruggeman, I. Melle, J. Arends, C. Arango and H. Knegtering (2017). "Treatment of negative symptoms: where do we stand, and where do we go?" Schizophrenia research **186**: 55-62.

Arancillo, M., S. W. Min, S. Gerber, A. Munster-Wandowski, Y. J. Wu, M. Herman, T. Trimbuch, J. C. Rah, G. Ahnert-Hilger, D. Riedel, T. C. Sudhof and C. Rosenmund (2013). "Titration of Syntaxin1 in mammalian synapses reveals multiple roles in vesicle docking, priming, and release probability." J Neurosci **33**(42): 16698-16714.

Asaka, Y., D. G. Jugloff, L. Zhang, J. H. Eubanks and R. M. Fitzsimonds (2006). "Hippocampal synaptic plasticity is impaired in the Mecp2-null mouse model of Rett syndrome." Neurobiol Dis **21**(1): 217-227.

Baker, K., S. L. Gordon, D. Grozeva, M. van Kogelenberg, N. Y. Roberts, M. Pike, E. Blair, M. E. Hurles, W. K. Chong, T. Baldeweg, M. A. Kurian, S. G. Boyd, M. A. Cousin and F. L. Raymond (2015). "Identification of a human synaptotagmin-1 mutation that perturbs synaptic vesicle cycling." J Clin Invest **125**(4): 1670-1678.

Baker, K., S. L. Gordon, H. Melland, F. Bumbak, D. J. Scott, T. J. Jiang, D. Owen, B. J. Turner, S. G. Boyd, M. Rossi, M. Al-Raqad, O. Elpeleg, D. Peck, G. M. S. Mancini, M. Wilke, M. Zollino, G. Marangi, H. Weigand, I. Borggraefe, T. Haack, Z. Stark, S. Sadedin, G. Broad Center for Mendelian, T. Y. Tan, Y.

Jiang, R. A. Gibbs, S. Ellingwood, M. Amaral, W. Kelley, M. A. Kurian, M. A. Cousin and F. L. Raymond (2018). "SYT1-associated neurodevelopmental disorder: a case series." Brain **141**(9): 2576-2591.

Bardy, C., M. van den Hurk, B. Kakaradov, J. A. Erwin, B. N. Jaeger, R. V. Hernandez, T. Eames, A. A. Paucar, M. Gorris, C. Marchand, R. Jappelli, J. Barron, A. K. Bryant, M. Kellogg, R. S. Lasken, B. P. Rutten, H. W. Steinbusch, G. W. Yeo and F. H. Gage (2016). "Predicting the functional states of human iPSC-derived neurons with single-cell RNA-seq and electrophysiology." Mol Psychiatry **21**(11): 1573-1588.

Basu, J., A. Betz, N. Brose and C. Rosenmund (2007). "Munc13-1 C1 domain activation lowers the energy barrier for synaptic vesicle fusion." J Neurosci **27**(5): 1200-1210.

Basu, J., N. Shen, I. Dulubova, J. Lu, R. Guan, O. Guryev, N. V. Grishin, C. Rosenmund and J. Rizo (2005). "A minimal domain responsible for Munc13 activity." Nat Struct Mol Biol **12**(11): 1017-1018.

Bekkers, J. M. and C. F. Stevens (1991). "Excitatory and inhibitory autaptic currents in isolated hippocampal neurons maintained in cell culture." Proc Natl Acad Sci U S A **88**(17): 7834-7838.

Bischofberger, J., D. Engel, L. Li, J. R. Geiger and P. Jonas (2006). "Patch-clamp recording from mossy fiber terminals in hippocampal slices." Nat Protoc **1**(4): 2075-2081.

Borst, J. G., F. Helmchen and B. Sakmann (1995). "Pre- and postsynaptic whole-cell recordings in the medial nucleus of the trapezoid body of the rat." J Physiol **489 (Pt 3)**: 825-840.

Bradberry, M. M., N. A. Courtney, M. J. Dominguez, S. M. Lofquist, A. T. Knox, R. B. Sutton and E. R. Chapman (2020). "Molecular Basis for Synaptotagmin-1-Associated Neurodevelopmental Disorder." Neuron **107**(1): 52-64 e57.

Brose, N., K. Hofmann, Y. Hata and T. C. Sudhof (1995). "Mammalian homologues of Caenorhabditis elegans unc-13 gene define novel family of C2-domain proteins." J Biol Chem **270**(42): 25273-25280.

Brose, N., A. G. Petrenko, T. C. Südhof and R. Jahn (1992). "Synaptotagmin: a calcium sensor on the synaptic vesicle surface." Science **256**(5059): 1021-1025.

Bruno, V., F. Caraci, A. Copani, F. Matrisciano, F. Nicoletti and G. Battaglia (2017). "The impact of metabotropic glutamate receptors into active neurodegenerative processes: a “dark side” in the development of new symptomatic treatments for neurologic and psychiatric disorders." Neuropharmacology **115**: 180-192.

Cadwell, C. R., A. Palasantza, X. Jiang, P. Berens, Q. Deng, M. Yilmaz, J. Reimer, S. Shen, M. Bethge and K. F. Tolias (2015). "Electrophysiological, transcriptomic and morphologic profiling of single neurons using Patch-seq." Nature biotechnology **34**(2): nbt. 3445.

Camacho, M., J. Basu, T. Trimbuch, S. Chang, C. Pulido-Lozano, S. S. Chang, I. Duluvova, M. Abo-Rady, J. Rizo and C. Rosenmund (2017). "Heterodimerization of Munc13 C2A domain with RIM regulates synaptic vesicle docking and priming." Nat Commun **8**: 15293.

Cases-Langhoff, C., B. Voss, A. M. Garner, U. Appeltauer, K. Takei, S. Kindler, R. W. Veh, P. De Camilli, E. D. Gundelfinger and C. C. Garner (1996). "Piccolo, a novel 420 kDa protein associated with the presynaptic cytomatrix." Eur J Cell Biol **69**(3): 214-223.

Chambers, S. M., C. A. Fasano, E. P. Papapetrou, M. Tomishima, M. Sadelain and L. Studer (2009). "Highly efficient neural conversion of human ES and iPS cells by dual inhibition of SMAD signaling." Nat Biotechnol **27**(3): 275-280.

Chanaday, N. L., M. A. Cousin, I. Milosevic, S. Watanabe and J. R. Morgan (2019). "The Synaptic Vesicle Cycle Revisited: New Insights into the Modes and Mechanisms." J Neurosci **39**(42): 8209-8216.

Chang, C. L., T. Trimbuch, H. T. Chao, J. C. Jordan, M. A. Herman and C. Rosenmund (2014). "Investigation of synapse formation and function in a glutamatergic-GABAergic two-neuron microcircuit." J Neurosci **34**(3): 855-868.

Chang, S., T. Trimbuch and C. Rosenmund (2018). "Synaptotagmin-1 drives synchronous Ca(2+)-triggered fusion by C2B-domain-mediated synaptic-vesicle-membrane attachment." Nat Neurosci **21**(1): 33-40.

Chao, H. T., H. Chen, R. C. Samaco, M. Xue, M. Chahrour, J. Yoo, J. L. Neul, S. Gong, H. C. Lu, N. Heintz, M. Ekker, J. L. Rubenstein, J. L. Noebels, C. Rosenmund and H. Y. Zoghbi (2010). "Dysfunction in GABA signalling mediates autism-like stereotypies and Rett syndrome phenotypes." Nature **468**(7321): 263-269.

Chao, H. T., H. Y. Zoghbi and C. Rosenmund (2007). "MeCP2 controls excitatory synaptic strength by regulating glutamatergic synapse number." Neuron **56**(1): 58-65.

Clayton, E. L. and M. A. Cousin (2009). "The molecular physiology of activity-dependent bulk endocytosis of synaptic vesicles." J Neurochem **111**(4): 901-914.

Clements, J. D. and J. M. Bekkers (1997). "Detection of spontaneous synaptic events with an optimally scaled template." Biophys J **73**(1): 220-229.

Colasante, G., G. Lignani, A. Rubio, L. Medrihan, L. Yekhlef, A. Sessa, L. Massimino, S. G. Giannelli, S. Sacchetti, M. Caiazzo, D. Leo, D. Alexopoulou, M. T. Dell'Anno, E. Ciabatti, M. Orlando, M. Studer, A. Dahl, R. R. Gainetdinov, S. Taverna, F. Benfenati and V. Broccoli (2015). "Rapid Conversion of

Fibroblasts into Functional Forebrain GABAergic Interneurons by Direct Genetic Reprogramming." Cell Stem Cell **17**(6): 719-734.

Comery, T. A., J. B. Harris, P. J. Willems, B. A. Oostra, S. A. Irwin, I. J. Weiler and W. T. Greenough (1997). "Abnormal dendritic spines in fragile X knockout mice: maturation and pruning deficits." Proc Natl Acad Sci U S A **94**(10): 5401-5404.

Conner, S. D. and S. L. Schmid (2003). "Regulated portals of entry into the cell." Nature **422**(6927): 37-44.

D'Aiuto, L., Y. Zhi, D. Kumar Das, M. R. Wilcox, J. W. Johnson, L. McClain, M. L. MacDonald, R. Di Maio, M. E. Schurdak, P. Piazza, L. Viggiano, R. Sweet, P. R. Kinchington, A. G. Bhattacharjee, R. Yolken and V. L. Nimgaonkar (2014). "Large-scale generation of human iPSC-derived neural stem cells/early neural progenitor cells and their neuronal differentiation." Organogenesis **10**(4): 365-377.

Delaney, K. R. and R. S. Zucker (1990). "Calcium released by photolysis of DM-nitrophen stimulates transmitter release at squid giant synapse." J Physiol **426**: 473-498.

Delvendahl, I., N. P. Vyleta, H. von Gersdorff and S. Hallermann (2016). "Fast, Temperature-Sensitive and Clathrin-Independent Endocytosis at Central Synapses." Neuron **90**(3): 492-498.

Denker, A. and S. O. Rizzoli (2010). "Synaptic vesicle pools: an update." Front Synaptic Neurosci **2**: 135.

Doherty, G. J. and H. T. McMahon (2009). "Mechanisms of endocytosis." Annu Rev Biochem **78**: 857-902.

Douglas, R. J. and K. A. Martin (2007). "Mapping the matrix: the ways of neocortex." Neuron **56**(2): 226-238.

Dresbach, T., B. Qualmann, M. M. Kessels, C. C. Garner and E. D. Gundelfinger (2001). "The presynaptic cytomatrix of brain synapses." Cell Mol Life Sci **58**(1): 94-116.

Duffney, L. J., P. Zhong, J. Wei, E. Matas, J. Cheng, L. Qin, K. Ma, D. M. Dietz, Y. Kajiwara, J. D. Buxbaum and Z. Yan (2015). "Autism-like Deficits in Shank3-Deficient Mice Are Rescued by Targeting Actin Regulators." Cell Rep **11**(9): 1400-1413.

Fatt, P. and B. Katz (1951). "An analysis of the end-plate potential recorded with an intracellular electrode." J Physiol **115**(3): 320-370.

Feldmeyer, D. (2012). "Excitatory neuronal connectivity in the barrel cortex." Front Neuroanat **6**: 24.

Fernandez-Chacon, R., A. Konigstorfer, S. H. Gerber, J. Garcia, M. F. Matos, C. F. Stevens, N. Brose, J. Rizo, C. Rosenmund and T. C. Sudhof (2001). "Synaptotagmin I functions as a calcium regulator of release probability." Nature **410**(6824): 41-49.

Forrest, M. P., H. Zhang, W. Moy, H. McGowan, C. Leites, L. E. Dionisio, Z. Xu, J. Shi, A. R. Sanders, W. J. Greenleaf, C. A. Cowan, Z. P. Pang, P. V. Gejman, P. Penzes and J. Duan (2017). "Open Chromatin Profiling in hiPSC-Derived Neurons Prioritizes Functional Noncoding Psychiatric Risk Variants and Highlights Neurodevelopmental Loci." Cell Stem Cell **21**(3): 305-318 e308.

Fromer, M., A. J. Pocklington, D. H. Kavanagh, H. J. Williams, S. Dwyer, P. Gormley, L. Georgieva, E. Rees, P. Palta, D. M. Ruderfer, N. Carrera, I. Humphreys, J. S. Johnson, P. Roussos, D. D. Barker, E. Banks, V. Milanova, S. G. Grant, E. Hannon, S. A. Rose, K. Chambert, M. Mahajan, E. M. Scolnick, J. L. Moran, G. Kirov, A. Palotie, S. A. McCarroll, P. Holmans, P. Sklar, M. J. Owen, S. M. Purcell and M. C. O'Donovan (2014). "De novo mutations in schizophrenia implicate synaptic networks." Nature **506**(7487): 179-184.

Furshpan, E. J. and D. D. Potter (1959). "Transmission at the giant motor synapses of the crayfish." J Physiol **145**(2): 289-325.

Geppert, M., Y. Goda, R. E. Hammer, C. Li, T. W. Rosahl, C. F. Stevens and T. C. Südhof (1994). "Synaptotagmin I: a major Ca2+ sensor for transmitter release at a central synapse." Cell **79**(4): 717-727.

Gunhanlar, N., G. Shpak, M. van der Kroeg, L. A. Gouty-Colomer, S. T. Munshi, B. Lendemeijer, M. Ghazvini, C. Dupont, W. J. G. Hoogendijk, J. Gribnau, F. M. S. de Vrij and S. A. Kushner (2018). "A simplified protocol for differentiation of electrophysiologically mature neuronal networks from human induced pluripotent stem cells." Mol Psychiatry **23**(5): 1336-1344.

Hammond, C. (2001). Cellular and Molecular Neurobiology, Academic Press.

Herman, M. A., F. Ackermann, T. Trimbuch and C. Rosenmund (2014). "Vesicular glutamate transporter expression level affects synaptic vesicle release probability at hippocampal synapses in culture." J Neurosci **34**(35): 11781-11791.

Hofker, M. H., J. Fu and C. Wijmenga (2014). "The genome revolution and its role in understanding complex diseases." Biochim Biophys Acta **1842**(10): 1889-1895.

Hook, V., K. J. Brennand, Y. Kim, T. Toneff, L. Funkelstein, K. C. Lee, M. Ziegler and F. H. Gage (2014). "Human iPSC neurons display activity-dependent neurotransmitter secretion: aberrant catecholamine levels in schizophrenia neurons." Stem Cell Reports **3**(4): 531-538.

Hormuzdi, S. G., M. A. Filippov, G. Mitropoulou, H. Monyer and R. Bruzzone (2004). "Electrical synapses: a dynamic signaling system that shapes the activity of neuronal networks." Biochim Biophys Acta **1662**(1-2): 113-137.

Huang, Y. and A. Thathiah (2015). "Regulation of neuronal communication by G protein-coupled receptors." FEBS Lett **589**(14): 1607-1619.

Hung, A. Y., K. Futai, C. Sala, J. G. Valtschanoff, J. Ryu, M. A. Woodworth, F. L. Kidd, C. C. Sung, T. Miyakawa, M. F. Bear, R. J. Weinberg and M. Sheng (2008). "Smaller dendritic spines, weaker synaptic transmission, but enhanced spatial learning in mice lacking Shank1." J Neurosci **28**(7): 1697-1708.

Jahn, R. and D. Fasshauer (2012). "Molecular machines governing exocytosis of synaptic vesicles." Nature **490**(7419): 201-207.

Jan, Y. N., L. Y. Jan and M. J. Dennis (1977). "Two mutations of synaptic transmission in Drosophila." Proc R Soc Lond B Biol Sci **198**(1130): 87-108.

Jiang, Y. H., D. Armstrong, U. Albrecht, C. M. Atkins, J. L. Noebels, G. Eichele, J. D. Sweatt and A. L. Beaudet (1998). "Mutation of the Angelman ubiquitin ligase in mice causes increased cytoplasmic p53 and deficits of contextual learning and long-term potentiation." Neuron **21**(4): 799-811.

Kandel, E. R., J. H. Schwartz and T. M. Jessell (2000). Principles of neural science, McGraw-hill New York.

Kim, S., D. Kim, S. W. Cho, J. Kim and J. S. Kim (2014). "Highly efficient RNA-guided genome editing in human cells via delivery of purified Cas9 ribonucleoproteins." Genome Res **24**(6): 1012-1019.

Ko, J., M. Na, S. Kim, J. R. Lee and E. Kim (2003). "Interaction of the ERC family of RIM-binding proteins with the liprin-alpha family of multidomain proteins." J Biol Chem **278**(43): 42377-42385.

Kononenko, N. L., D. Puchkov, G. A. Classen, A. M. Walter, A. Pechstein, L. Sawade, N. Kaempf, T. Trimbuch, D. Lorenz, C. Rosenmund, T. Maritzen and V. Haucke (2014). "Clathrin/AP-2 mediate synaptic vesicle reformation from endosome-like vacuoles but are not essential for membrane retrieval at central synapses." Neuron **82**(5): 981-988.

Kouser, M., H. E. Speed, C. M. Dewey, J. M. Reimers, A. J. Widman, N. Gupta, S. Liu, T. C. Jaramillo, M. Bangash, B. Xiao, P. F. Worley and C. M. Powell

(2013). "Loss of predominant Shank3 isoforms results in hippocampus-dependent impairments in behavior and synaptic transmission." J Neurosci **33**(47): 18448-18468.

Larsen, W. J. (1977). "Structural diversity of gap junctions. A review." Tissue Cell **9**(3): 373-394.

Li, L., O. H. Shin, J. S. Rhee, D. Arac, J. C. Rah, J. Rizo, T. Sudhof and C. Rosenmund (2006). "Phosphatidylinositol phosphates as co-activators of Ca2+ binding to C2 domains of synaptotagmin 1." J Biol Chem **281**(23): 15845-15852.

Liang, G. and Y. Zhang (2013). "Genetic and epigenetic variations in iPSCs: potential causes and implications for application." Cell Stem Cell **13**(2): 149-159.

Lipstein, N., N. M. Verhoeven-Duif, F. E. Michelassi, N. Calloway, P. M. van Hasselt, K. Pienkowska, G. van Haaften, M. M. van Haelst, R. van Empelen, I. Cuppen, H. C. van Teeseling, A. M. Evelein, J. A. Vorstman, S. Thoms, O. Jahn, K. J. Duran, G. R. Monroe, T. A. Ryan, H. Taschenberger, J. S. Dittman, J. S. Rhee, G. Visser, J. J. Jans and N. Brose (2017). "Synaptic UNC13A protein variant causes increased neurotransmission and dyskinetic movement disorder." J Clin Invest **127**(3): 1005-1018.

Liu, H., E. R. Chapman and C. Dean (2013). ""Self" versus "non-self" connectivity dictates properties of synaptic transmission and plasticity." PLoS One **8**(4): e62414.

Lois, C., E. J. Hong, S. Pease, E. J. Brown and D. Baltimore (2002). "Germline transmission and tissue-specific expression of transgenes delivered by lentiviral vectors." Science **295**(5556): 868-872.

Mangan, P. S. and J. Kapur (2004). "Factors underlying bursting behavior in a network of cultured hippocampal neurons exposed to zero magnesium." J Neurophysiol **91**(2): 946-957.

Meijer, M., K. Rehbach, J. W. Brunner, J. A. Classen, H. C. A. Lammertse, L. A. van Linge, D. Schut, T. Krutenko, M. Hebisch, L. N. Cornelisse, P. F. Sullivan, M. Peitz, R. F. Toonen, O. Brustle and M. Verhage (2019). "A Single-Cell Model for Synaptic Transmission and Plasticity in Human iPSC-Derived Neurons." Cell Rep **27**(7): 2199-2211 e2196.

Mertens, J., Q. W. Wang, Y. Kim, D. X. Yu, S. Pham, B. Yang, Y. Zheng, K. E. Diffenderfer, J. Zhang, S. Soltani, T. Eames, S. T. Schafer, L. Boyer, M. C. Marchetto, J. I. Nurnberger, J. R. Calabrese, K. J. Odegaard, M. J. McCarthy, P. P. Zandi, M. Alda, C. M. Nievergelt, S. Pharmacogenomics of Bipolar Disorder, S. Mi, K. J. Brennand, J. R. Kelsoe, F. H. Gage and J. Yao (2015). "Differential responses to lithium in hyperexcitable neurons from patients with bipolar disorder." Nature **527**(7576): 95-99.

Michalon, A., M. Sidorov, T. M. Ballard, L. Ozmen, W. Spooren, J. G. Wettstein, G. Jaeschke, M. F. Bear and L. Lindemann (2012). "Chronic pharmacological mGlu5 inhibition corrects fragile X in adult mice." Neuron **74**(1): 49-56.

Miyamoto, S., N. Miyake, L. F. Jarskog, W. W. Fleischhacker and J. A. Lieberman (2012). "Pharmacological treatment of schizophrenia: a critical review of the pharmacology and clinical effects of current and future therapeutic agents." Mol Psychiatry **17**(12): 1206-1227.

Morton, A., J. R. Marland and M. A. Cousin (2015). "Synaptic vesicle exocytosis and increased cytosolic calcium are both necessary but not sufficient for activity-dependent bulk endocytosis." J Neurochem **134**(3): 405-415.

Moyer, J. R., Jr. and T. H. Brown (1998). "Methods for whole-cell recording from visually preselected neurons of perirhinal cortex in brain slices from young and aging rats." J Neurosci Methods **86**(1): 35-54.

Murthy, V. N., T. Schikorski, C. F. Stevens and Y. Zhu (2001). "Inactivity produces increases in neurotransmitter release and synapse size." Neuron **32**(4): 673-682.

Neher, E. and A. Marty (1982). "Discrete changes of cell membrane capacitance observed under conditions of enhanced secretion in bovine adrenal chromaffin cells." Proc Natl Acad Sci U S A **79**(21): 6712-6716.

Ohtsuka, T., E. Takao-Rikitsu, E. Inoue, M. Inoue, M. Takeuchi, K. Matsubara, M. Deguchi-Tawarada, K. Satoh, K. Morimoto, H. Nakanishi and Y. Takai (2002). "Cast: a novel protein of the cytomatrix at the active zone of synapses that forms a ternary complex with RIM1 and munc13-1." J Cell Biol **158**(3): 577-590.

Pak, C., T. Danko, Y. Zhang, J. Aoto, G. Anderson, S. Maxeiner, F. Yi, M. Wernig and T. C. Sudhof (2015). "Human Neuropsychiatric Disease Modeling using Conditional Deletion Reveals Synaptic Transmission Defects Caused by Heterozygous Mutations in NRXN1." Cell Stem Cell **17**(3): 316-328.

Patzke, C., C. Acuna, L. R. Giam, M. Wernig and T. C. Sudhof (2016). "Conditional deletion of L1CAM in human neurons impairs both axonal and dendritic arborization and action potential generation." J Exp Med **213**(4): 499-515.

Patzke, C., Y. Han, J. Covy, F. Yi, S. Maxeiner, M. Wernig and T. C. Sudhof (2015). "Analysis of conditional heterozygous STXBP1 mutations in human neurons." J Clin Invest **125**(9): 3560-3571.

Pereda, A. E. (2014). "Electrical synapses and their functional interactions with chemical synapses." Nat Rev Neurosci **15**(4): 250-263.

Pratt, K. G., P. Zhu, H. Watari, D. G. Cook and J. M. Sullivan (2011). "A novel role for {gamma}-secretase: selective regulation of spontaneous neurotransmitter release from hippocampal neurons." J Neurosci **31**(3): 899-906.

Priller, C., I. Dewachter, N. Vassallo, S. Paluch, C. Pace, H. A. Kretzschmar, F. Van Leuven and J. Herms (2007). "Mutant presenilin 1 alters synaptic transmission in cultured hippocampal neurons." J Biol Chem **282**(2): 1119-1127.

Purcell, S. M., J. L. Moran, M. Fromer, D. Ruderfer, N. Solovieff, P. Roussos, C. O'Dushlaine, K. Chambert, S. E. Bergen, A. Kahler, L. Duncan, E. Stahl, G. Genovese, E. Fernandez, M. O. Collins, N. H. Komiyama, J. S. Choudhary, P. K. Magnusson, E. Banks, K. Shakir, K. Garimella, T. Fennell, M. DePristo, S. G. Grant, S. J. Haggarty, S. Gabriel, E. M. Scolnick, E. S. Lander, C. M. Hultman, P. F. Sullivan, S. A. McCarroll and P. Sklar (2014). "A polygenic burden of rare disruptive mutations in schizophrenia." Nature **506**(7487): 185-190.

Rhee, H. J., A. H. Shaib, K. Rehbach, C. Lee, P. Seif, C. Thomas, E. Gideons, A. Guenther, T. Krutenko, M. Hebisch, M. Peitz, N. Brose, O. Brustle and J. S. Rhee (2019). "An Autaptic Culture System for Standardized Analyses of iPSC-Derived Human Neurons." Cell Rep **27**(7): 2212-2228 e2217.

Rhee, J. S., A. Betz, S. Pyott, K. Reim, F. Varoqueaux, I. Augustin, D. Hesse, T. C. Sudhof, M. Takahashi, C. Rosenmund and N. Brose (2002). "Beta phorbol ester- and diacylglycerol-induced augmentation of transmitter release is mediated by Munc13s and not by PKCs." Cell **108**(1): 121-133.

Rhee, J. S., L. Y. Li, O. H. Shin, J. C. Rah, J. Rizo, T. C. Sudhof and C. Rosenmund (2005). "Augmenting neurotransmitter release by enhancing the apparent Ca2+ affinity of synaptotagmin 1." Proc Natl Acad Sci U S A **102**(51): 18664-18669.

Rizo, J. and C. Rosenmund (2008). "Synaptic vesicle fusion." Nature structural & molecular biology **15**(7): 665-674.

Rizzoli, S. O. (2014). "Synaptic vesicle recycling: steps and principles." EMBO J **33**(8): 788-822.

Rizzoli, S. O. and W. J. Betz (2005). "Synaptic vesicle pools." Nat Rev Neurosci **6**(1): 57-69.

Rosenmund, C. and C. F. Stevens (1996). "Definition of the readily releasable pool of vesicles at hippocampal synapses." Neuron **16**(6): 1197-1207.

Saheki, Y. and P. De Camilli (2012). "Synaptic vesicle endocytosis." Cold Spring Harb Perspect Biol **4**(9): a005645.

Sampathkumar, C., Y. J. Wu, M. Vadhvani, T. Trimbuch, B. Eickholt and C. Rosenmund (2016). "Loss of MeCP2 disrupts cell autonomous and autocrine BDNF signaling in mouse glutamatergic neurons." Elife **5**.

Scanziani, M., M. Capogna, B. H. Gahwiler and S. M. Thompson (1992). "Presynaptic inhibition of miniature excitatory synaptic currents by baclofen and adenosine in the hippocampus." Neuron **9**(5): 919-927.

Schikorski, T. and C. F. Stevens (1997). "Quantitative ultrastructural analysis of hippocampal excitatory synapses." J Neurosci **17**(15): 5858-5867.

Schmeisser, M. J., E. Ey, S. Wegener, J. Bockmann, A. V. Stempel, A. Kuebler, A. L. Janssen, P. T. Udvardi, E. Shiban, C. Spilker, D. Balschun, B. V. Skryabin, S. Dieck, K. H. Smalla, D. Montag, C. S. Leblond, P. Faure, N. Torquet, A. M. Le Sourd, R. Toro, A. M. Grabrucker, S. A. Shoichet, D. Schmitz, M. R. Kreutz, T. Bourgeron, E. D. Gundelfinger and T. M. Boeckers (2012). "Autistic-like behaviours and hyperactivity in mice lacking ProSAP1/Shank2." Nature **486**(7402): 256-260.

Schotten, S., M. Meijer, A. M. Walter, V. Huson, L. Mamer, L. Kalogreades, M. ter Veer, M. Ruiter, N. Brose, C. Rosenmund, J. B. Sorensen, M. Verhage and L. N. Cornelisse (2015). "Additive effects on the energy barrier for synaptic vesicle fusion cause supralinear effects on the vesicle fusion rate." Elife **4**: e05531.

Serra-Pages, C., Q. G. Medley, M. Tang, A. Hart and M. Streuli (1998). "Liprins, a family of LAR transmembrane protein-tyrosine phosphatase-interacting proteins." J Biol Chem **273**(25): 15611-15620.

Shi, Y., P. Kirwan and F. J. Livesey (2012). "Directed differentiation of human pluripotent stem cells to cerebral cortex neurons and neural networks." Nat Protoc **7**(10): 1836-1846.

Shin, O. H., J. Lu, J. S. Rhee, D. R. Tomchick, Z. P. Pang, S. M. Wojcik, M. Camacho-Perez, N. Brose, M. Machius, J. Rizo, C. Rosenmund and T. C. Sudhof (2010). "Munc13 C2B domain is an activity-dependent Ca2+ regulator of synaptic exocytosis." Nat Struct Mol Biol **17**(3): 280-288.

Sudhof, T. C. (2004). "The synaptic vesicle cycle." Annu Rev Neurosci **27**: 509-547.

Sudhof, T. C. and R. Jahn (1991). "Proteins of synaptic vesicles involved in exocytosis and membrane recycling." Neuron **6**(5): 665-677.

Sudhof, T. C. and J. Rizo (2011). "Synaptic vesicle exocytosis." Cold Spring Harb Perspect Biol **3**(12).

Ting, J. T., B. G. Kelley, T. J. Lambert, D. G. Cook and J. M. Sullivan (2007). "Amyloid precursor protein overexpression depresses excitatory transmission through both presynaptic and postsynaptic mechanisms." Proc Natl Acad Sci U S A **104**(1): 353-358.

tom Dieck, S., L. Sanmarti-Vila, K. Langnaese, K. Richter, S. Kindler, A. Soyke, H. Wex, K. H. Smalla, U. Kampf, J. T. Franzer, M. Stumm, C. C. Garner and E. D. Gundelfinger (1998). "Bassoon, a novel zinc-finger CAG/glutamine-repeat protein selectively localized at the active zone of presynaptic nerve terminals." J Cell Biol **142**(2): 499-509.

Trimbuch, T., J. Xu, D. Flaherty, D. R. Tomchick, J. Rizo and C. Rosenmund (2014). "Re-examining how complexin inhibits neurotransmitter release." Elife **3**: e02391.

Valtorta, F., J. Meldolesi and R. Fesce (2001). "Synaptic vesicles: is kissing a matter of competence?" Trends Cell Biol **11**(8): 324-328.

Van Der Loos, H. and E. M. Glaser (1972). "Autapses in neocortex cerebri: synapses between a pyramidal cell's axon and its own dendrites." Brain Research **48**: 355-360.

Varoqueaux, F., A. Sigler, J. S. Rhee, N. Brose, C. Enk, K. Reim and C. Rosenmund (2002). "Total arrest of spontaneous and evoked synaptic transmission but normal synaptogenesis in the absence of Munc13-mediated vesicle priming." Proc Natl Acad Sci U S A **99**(13): 9037-9042.

Vierbuchen, T., A. Ostermeier, Z. P. Pang, Y. Kokubu, T. C. Sudhof and M. Wernig (2010). "Direct conversion of fibroblasts to functional neurons by defined factors." Nature **463**(7284): 1035-1041.

Wang, Y., X. Liu, T. Biederer and T. C. Sudhof (2002). "A family of RIM-binding proteins regulated by alternative splicing: Implications for the genesis of synaptic active zones." Proc Natl Acad Sci U S A **99**(22): 14464-14469.

Wang, Y., M. Okamoto, F. Schmitz, K. Hofmann and T. C. Sudhof (1997). "Rim is a putative Rab3 effector in regulating synaptic-vesicle fusion." Nature **388**(6642): 593-598.

Wang, Y. and T. C. Sudhof (2003). "Genomic definition of RIM proteins: evolutionary amplification of a family of synaptic regulatory proteins." Genomics **81**(2): 126-137.

Wang, Y., S. Sugita and T. C. Sudhof (2000). "The RIM/NIM family of neuronal C2 domain proteins. Interactions with Rab3 and a new class of Src homology 3 domain proteins." J Biol Chem **275**(26): 20033-20044.

Watanabe, S., B. R. Rost, M. Camacho-Perez, M. W. Davis, B. Sohl-Kielczynski, C. Rosenmund and E. M. Jorgensen (2013). "Ultrafast endocytosis at mouse hippocampal synapses." Nature **504**(7479): 242-247.

Watanabe, S., T. Trimbuch, M. Camacho-Perez, B. R. Rost, B. Brokowski, B. Sohl-Kielczynski, A. Felies, M. W. Davis, C. Rosenmund and E. M. Jorgensen (2014). "Clathrin regenerates synaptic vesicles from endosomes." Nature **515**(7526): 228-233.

Weber, T., B. V. Zemelman, J. A. McNew, B. Westermann, M. Gmachl, F. Parlati, T. H. Sollner and J. E. Rothman (1998). "SNAREpins: minimal machinery for membrane fusion." Cell **92**(6): 759-772.

Wenzel, E. M., A. Morton, K. Ebert, O. Welzel, J. Kornhuber, M. A. Cousin and T. W. Groemer (2012). "Key physiological parameters dictate triggering of activity-dependent bulk endocytosis in hippocampal synapses." PLoS One **7**(6): e38188.

Weston, M. C., H. Chen and J. W. Swann (2014). "Loss of mTOR repressors Tsc1 or Pten has divergent effects on excitatory and inhibitory synaptic transmission in single hippocampal neuron cultures." Front Mol Neurosci **7**: 1.

Weston, M. C., R. B. Nehring, S. M. Wojcik and C. Rosenmund (2011). "Interplay between VGLUT isoforms and endophilin A1 regulates neurotransmitter release and short-term plasticity." Neuron **69**(6): 1147-1159.

Wierda, K. D. and J. B. Sorensen (2014). "Innervation by a GABAergic neuron depresses spontaneous release in glutamatergic neurons and unveils the clamping phenotype of synaptotagmin-1." J Neurosci **34**(6): 2100-2110.

Wu, X. S., S. H. Lee, J. Sheng, Z. Zhang, W. D. Zhao, D. Wang, Y. Jin, P. Charnay, J. M. Ervasti and L. G. Wu (2016). "Actin Is Crucial for All Kinetically Distinguishable Forms of Endocytosis at Synapses." Neuron **92**(5): 1020-1035.

Xue, M., C. Ma, T. K. Craig, C. Rosenmund and J. Rizo (2008). "The Janus-faced nature of the C(2)B domain is fundamental for synaptotagmin-1 function." Nat Struct Mol Biol **15**(11): 1160-1168.

Yi, F., T. Danko, S. C. Botelho, C. Patzke, C. Pak, M. Wernig and T. C. Sudhof (2016). "Autism-associated SHANK3 haploinsufficiency causes Ih channelopathy in human neurons." Science **352**(6286): aaf2669.

Young-Pearse, T. L. and E. M. Morrow (2016). "Modeling developmental neuropsychiatric disorders with iPSC technology: challenges and opportunities." Curr Opin Neurobiol **36**: 66-73.

Yuste, R. (2015). "From the neuron doctrine to neural networks." Nat Rev Neurosci **16**(8): 487-497.

Zhang, Y., C. Pak, Y. Han, H. Ahlenius, Z. Zhang, S. Chanda, S. Marro, C. Patzke, C. Acuna, J. Covy, W. Xu, N. Yang, T. Danko, L. Chen, M. Wernig and T. C. Sudhof (2013). "Rapid single-step induction of functional neurons from human pluripotent stem cells." Neuron **78**(5): 785-798.

Zhen, M. and Y. Jin (1999). "The liprin protein SYD-2 regulates the differentiation of presynaptic termini in C. elegans." Nature **401**(6751): 371-375.

Mein Lebenslauf wird aus datenschutzrechtlichen Gründen in der elektronischen Version nicht veröffentlicht.

Mein Lebenslauf wird aus datenschutzrechtlichen Gründen in der elektronischen Version nicht veröffentlicht.

Appendix

Statement of Contributions

If not stated differently experiments were carried out by me. Measurements of morphological parameters of human iNs was performed Dr. Katharina Grauel and Dr. Anja Dorrn. Electrophysiological recordings of evoked NT release for the initial characterization was done in collaboration by Dr. Katharina Grauel, Dr. Anja Dorrn and me. Characterization of the UNC 13 A KD was done in collaboration by Dr. Katharina Grauel, Marisa Brockmann and me. Experimental designs by Prof. Dr. Christian Rosenmund and me.

Preparation of astrocyte feeder cultures was done in collaboration by Rike Dannenberg, Heike Lerch and me. Microdot stamping was performed by Rike Dannenberg and Heike Lerch. Experimental design of lentiviral constructs was organized and instructed by Dr. Thorsten Trimbuch and carried out by Katja Pötschke and Bettina Brokowski. Maintenance of iPSCs was performed by Katja Pötschke. The above mentioned are all members of the Rosenmund laboratory.

Publications

Patzke, C., M. M. Brockmann, J. Dai, K. J. Gan, M. K. Grauel, **P. Fenske**, Y. Liu, C. Acuna, C. Rosenmund and T. C. Sudhof (2019). "Neuromodulator Signaling Bidirectionally Controls Vesicle Numbers in Human Synapses." Cell 179(2): 498-513 e422.

Fenske, P. and C. Rosenmund (2019). "A Single Human Neuron Approach to Synapse Function." Trends Mol Med 25(7): 563-565.

Fenske, P., M. K. Grauel, M. M. Brockmann, A. L. Dorrn, T. Trimbuch and C. Rosenmund (2019). "Autaptic cultures of human induced neurons as a versatile platform for studying synaptic function and neuronal morphology." Sci Rep 9(1): 4890.

Watanabe, S., L. E. Mamer, S. Raychaudhuri, D. Luvsanjav, J. Eisen, T. Trimbuch, B. Sohl-Kielczynski, **P. Fenske**, I. Milosevic, C. Rosenmund and E. M. Jorgensen (2018). "Synaptojanin and Endophilin Mediate Neck Formation during Ultrafast Endocytosis." Neuron 98(6): 1184-1197 e1186.

Piwecka, M., P. Glazar, L. R. Hernandez-Miranda, S. Memczak, S. A. Wolf, A. Rybak-Wolf, A. Filipchyk, F. Klironomos, C. A. Cerda Jara, **P. Fenske**, T. Trimbuch, V. Zywitza, M. Plass, L. Schreyer, S. Ayoub, C. Kocks, R. Kuhn, C. Rosenmund, C. Birchmeier and N. Rajewsky (2017). "Loss of a mammalian circular RNA locus causes miRNA deregulation and affects brain function." Science 357(6357).

Klar, M., **P. Fenske**, F. R. Vega, C. Dame and A. U. Brauer (2015). "Transcription factor Yin-Yang 2 alters neuronal outgrowth in vitro." Cell Tissue Res 362(2): 453-460.

Poster Presentations

Human induced neuronal autaptic cultures to study synaptic function and neuronal morphology. Society for Neuroscience International Conference (Chicago, USA, October 2019)

Studying synaptic function and neuronal morphology by human induced neuronal autaptic cultures. FENS Forum of Neuroscience (Berlin, Germany, July 2018)